Anti-interferon auto-antibodies: effect of inhibition of the interferon system on influenza A virus replication *in vitro*

by

C. M. (Marijn) de Heer

Research Project Report

15-11-2023

Research Project Performed in Prof. Dr. Benjamin G. Hale Group, Institute of Medical Virology, University of Zurich

Research Project Supervised by Dr. Kevin Groen

Abstract

The innate immune response is the first line of defense against viral infections. Upon infection, viruses are sensed by cells which triggers a signaling cascade that leads to the production of interferons (IFNs). IFNs induce the expression of IFN-stimulated genes, thereby causing cells to enter an antiviral state. Recently, auto-antibodies (auto-Abs) neutralizing the antiviral activity of IFNs have been detected in patients suffering from severe viral diseases, and these anti-IFN auto-Abs have been associated with disease severity caused by several viruses. To better understand the molecular mechanisms of anti-IFN auto-Abs and their relationship to virus replication, an initial *in vitro* model system to study the effect of inhibition of the IFN system on influenza A virus (IAV) replication was developed, involving A549 cells and the avian IAV A/mallard/New York/6750/1978 (A/mallard/NY/78). In addition, tools and assays were set-up with the aim of studying the effect of anti-IFN auto-Abs on virus replication *in vitro*. Replication of A/mallard/NY/78 was enhanced upon treatment of A549 cells with ruxolitinib (a JAK inhibitor). In contrast, no consistent enhancement of A/mallard/NY/78-replication was observed in A549 cells treated with anti-IFNAR and/or anti-IFNLR Abs. Next, an anti-IFNα auto-Ab was cloned and produced, and commercial neutralizing Abs against IFNα, IFNß, and IFNω were characterized. Additionally, CRISPR/Cas9-mediated knockout of *IFNAR1, IFNLR1*, and type I IFNs was performed. The genomic, functional and western blot data of selected *IFNAR1* and *IFNLR1* single cell clones showed inconsistencies, and further validation of individual single cell knockout clones is therefore required. Initial virus replication kinetics experiments with A/mallard/NY/78 and GFP-expressing viruses in *IFNAR1* and *IFNLR1* single cell knockout clones did not show enhanced virus replication compared to wild-type A549 2D8 cells. Overall, this report described efforts to set-up assays and a model system to elucidate the molecular characteristics of anti-IFN auto-Abs and their relationship to virus replication.

Plain Language Summary

The innate immune response is the first line of defense against viral infections. Upon infection, viruses are sensed by the cell which triggers a signaling cascade that leads to the production and secretion of interferons (IFNs). These small proteins bind to the IFN receptor and activate the production of hundreds of IFN-stimulated genes (ISGs) in neighboring cells. ISGs are proteins that inhibit virus replication at all different steps of the viral replication cycle, thereby causing cells to enter an antiviral state and control viral infection. There are three types of IFNs: type I, type II, and type III IFNs. The subdivision is based on receptor usage. Type I and III IFNs are mainly responsible for the activation of the antiviral state, whereas type II IFN plays a role in activating adaptive immune cells. Recently, auto-antibodies (auto-Abs) neutralizing the antiviral activity of IFNs have been detected in patients suffering from severe viral diseases, including coronavirus disease 2019 (COVID-19) and influenza pneumonia. These anti-IFN auto-Abs are directed against the body's own proteins, and should therefore not be developed. The presence of anti-IFN auto-Abs is associated with disease severity caused by several viruses. At the moment, little is known about the molecular characteristics of anti-IFN auto-Abs. To better understand the molecular mechanisms of anti-IFN auto-Abs and their relationship to virus replication, an initial model system was set-up to study the effect of inhibition of the IFN system on influenza A virus (IAV) replication. The avian IAV A/mallard/New York/6750/1978 (A/mallard/NY/78) was selected as the model virus, as replication of this virus was restricted by IFNs. Next, enhanced A/mallard/NY/78-replication was observed when cells were treated with an inhibitor of the IFN signaling pathway. This showed that complete blockage of the IFN system resulted in enhanced replication of A/mallard/NY/78. In contrast, no consistent enhancement of A/mallard/NY/78-replication was observed when the type I and/or type III IFN receptor was blocked with antibodies. Due to these inconsistent results, further optimization of the initial model system is needed. In addition, an anti-IFN auto-Ab was produced in-house, and commercial Abs neutralizing different type I IFNs were characterized. These neutralizing Abs can be used to study the effect of blockage of individual IFNs on virus replication in the future. Furthermore, successful gene knockout of type I IFNs, the type I IFN receptor, and the type III IFN receptor was performed. Several assays were performed to validate the knockout cell lines, which showed inconsistencies and optimization is therefore required. The knockout cell lines can be used to study the effect of the type I and type III IFN system on the replication of (influenza A) viruses. Overall, this report described efforts to set-up assays and a model system to study the effect of inhibition of the IFN system on IAV replication. Further optimization is needed before these assays and the model system can be used to elucidate the molecular characteristics of anti-IFN auto-Abs and their relationship to virus replication.

Table of Contents

Introduction

The innate immune response is the first line of defense against viral infections (*1*). Upon detection of pathogen-associated molecular patterns (PAMPs) by the host's pattern recognition receptors (PRRs), a signaling cascade is activated that results in the activation of an immune response towards a virus (**Fig. 1**) (*2*). For many viral infections, this leads to the production of interferons (IFNs) (*1*, *3*, *4*). IFNs are a group of cytokines that act as signaling molecules, thereby triggering antiviral defenses in cells (*2*). IFNs do this by inducing the transcription of hundreds of IFN-stimulated genes (ISGs), causing cells to enter an antiviral state (*1*). ISGs encode proteins that inhibit virus replication at all different steps of the viral replication cycle (*5*). There are three types of IFNs: type I IFNs (13 IFNαs (IFNα1, α2, α4, α5, α6, α7, α8, α10, α13, α14, α16, α17, α21), IFNß, IFNε, IFNκ and IFNω), type II IFN (IFNγ), and type III IFNs (IFNλ1, λ2, λ3, λ4) (*1*, *2*). The subdivision is based on receptor usage (*1*). Type I IFNs use the heterodimeric IFN alpha receptor (IFNAR), consisting of the subunits IFNAR1 and IFNAR2, the IFN gamma receptor (IFNGR) (consisting of the IFNGR1 and IFNGR2 subunits) is used by type II IFN, and the IFN lambda receptor (IFNLR), consisting of IFNLR1 and IL-10Rb, is used by type III IFNs (*6*, *7*). Type I and III IFNs are mainly responsible for the activation of the antiviral state, whereas type II IFN plays a role in activating macrophages and adaptive immune cells (*1*, *8*, *9*). In this report, the focus is on type I and type III IFNs. Once type I IFNs or type III IFNs bind their respective receptor, IFN signaling is activated (**Fig. 1**) (*6*). This involves the activation of the Tyrosine Kinase 2 (TYK2) and Janus Kinase 1 (JAK1) kinases, the phosphorylation of Signal Transducer And Activator Of Transcription 1 (STAT1) and STAT2, further downstream signaling, and subsequently the expression of hundreds of ISGs, potentially resulting in the restriction of virus replication (*6*).

The importance of IFNs in restricting viral infections has been well described, as it is well known that human inborn errors of IFNs and the IFN signaling pathway can underlie viral diseases (*10*). This does not only include defunct proteins involved in the IFN signaling cascade (*e.g.* STAT1 or IFNAR1 deficiency (*11*, *12*)), but also auto-antibodies (Abs) against IFNs (*9*, *10*, *13*). The role of these anti-IFN auto-Abs

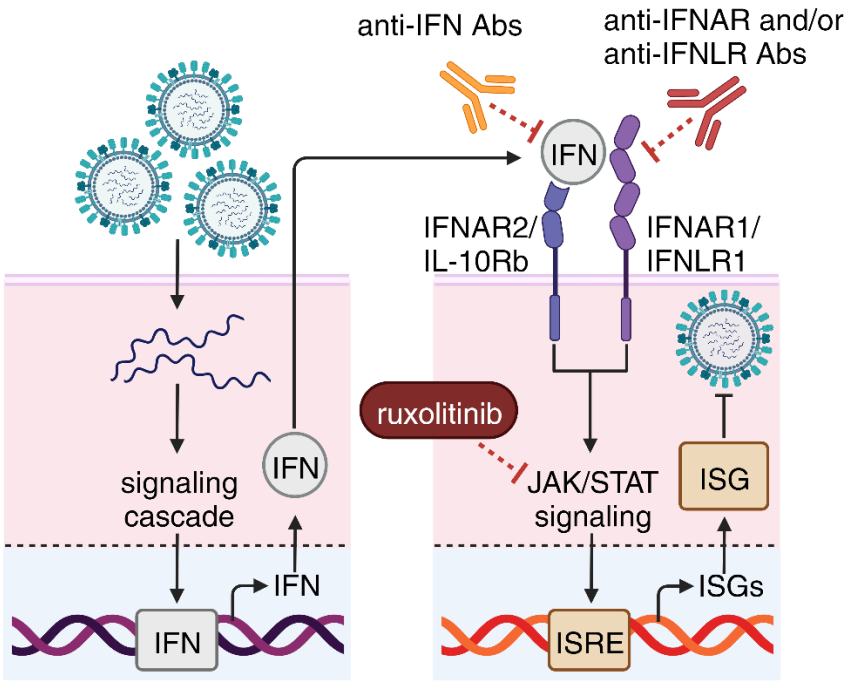

Fig. 1. Schematic representation of inhibitors of IFN signaling used in this study. Schematic overview of the IFN system. IFN signaling can be inhibited at different levels. Complete IFN signaling can be blocked by ruxolitinib (a JAK inhibitor), anti-IFNAR and anti-IFNLR Abs can be used to block type I IFN and type III IFN signaling, respectively, and anti-IFNs Abs can be used to block individual IFNs. ISRE: interferon-stimulated response element. Created with BioRender.com.

became more apparent during the coronavirus disease 2019 (COVID-19) pandemic, the disease caused by severe acute respiratory syndrome coronavirus 2 (SARS-CoV-2) (*10*). It was shown that around 10% of severe COVID-19 patients and 20% of people dying from COVID-19 had anti-type I IFN auto-Abs (*10*, *14*–*19*). Anti-type I IFN auto-Abs have not only been observed in severe COVID-19 patients but have also been detected in about 5% of life-threatening influenza pneumonia patients younger than 70 years old, around 40% of patients with West Nile Virus (WNV) encephalitis, 30% of people with severe adverse reactions to the yellow fever vaccine, and in patients with other viral diseases (*20*–*23*). These IFN auto-Abs are also present in the general human population (*14*). Anti-IFNα and/or anti-IFNω auto-Abs could be detected in 0.2% of humans between 18 and 69 years, 1.1% for 70–79-year-olds, and 3.4% of people aged 80 and older in a study conducted in 2020 and 2021 (*14*).

Despite the renewed and increased interest in anti-IFN auto-Abs, there is very little known about the molecular characteristics of them (*24*). Current knowledge is limited to the percentage of detectable anti-IFN auto-Abs in the general population and the percentage of patients with different viral diseases harboring these auto-Abs. In addition, it has been noted that anti-type I IFN auto-Abs are more commonly targeted against IFNα and IFNω, and less against IFNß (*14*). Furthermore, it is known that the percentage of neutralizing anti-type III IFN auto-Abs in severe COVID-19 patients is very low, and that these auto-Abs do not seem to predispose to severe COVID-19 (*25*). Any knowledge on the molecular mechanisms of anti-IFN auto-Abs is missing. For example, it is not known how these anti-IFN auto-Abs are developed, whether anti-IFN auto-Abs enhance viral replication and/or viral disease susceptibility, and why certain IFNs are more commonly targeted than others. Furthermore, it is not known how anti-IFN auto-Abs against only one IFN protein may already lead to increased viral disease susceptibility (*24*). The most straightforward mechanism of how these anti-IFN auto-Abs could promote viral replication is that these auto-Abs bind and neutralize IFNs, thereby blocking the IFN-IFN receptor interaction, which prevents the upregulation of ISG expression, ultimately leading to increased viral replication (*24*). Nevertheless, it is still unknown whether this is the molecular mechanism that leads to increased viral replication and disease susceptibility. Other research groups tried to elucidate the molecular mechanism of these anti-IFN auto-Abs by adding a pre-incubated mixture of anti-IFN auto-Abs (in patient serum) and type I IFNs before or shortly after inoculating cells with SARS-CoV-2, Middle East respiratory syndrome coronavirus (MERS-CoV), lymphocytic choriomeningitis virus (LCMV), WNV or IAV (*20*, *26*–*29*). In all studies, anti-IFN auto-Abs abrogated the inhibitory effect of type I IFNs on viral replication (*20*, *26*–*29*). However, in all studies exogenous IFN was added, and therefore it is currently not known whether relevant levels of anti-IFN auto-Abs can neutralize endogenously produced IFNs in an *in vitro* model, and how these anti-IFN auto-Abs might influence viral replication (*20*, *26*–*29*). To better understand the molecular mechanisms of these anti-IFN auto-Abs and their relationship to virus replication, an *in vitro* model was set-up involving human lung tissue cell lines and avian influenza A virus (IAV). This model system was used to study the effect of inhibition of the IFN system on IAV replication *in vitro*, the aim of the study. Furthermore, the model was used to determine which IFNs are produced upon virus infection, and thereby it was established which IFNs need to blocked to enhance IAV replication. The *in vitro* model system could be used in follow-up experiments to answer the question whether anti-IFN auto-Abs increase viral replication *in vitro*, and if so, which specific anti-IFN auto-Abs enhance viral replication? What levels of anti-IFN auto-Abs are required for increased viral replication, and lastly, do anti-IFN auto-Abs lead to viral persistence and thereby result in increased virus evolution?

This report describes the development of an initial *in vitro* model to study the effect of inhibition of the IFN system on IAV replication. Several IFN-sensitive IAVs were identified in a pilot experiment, and the avian IAV A/mallard/New York/6750/1978 (A/mallard/NY/78; H2N2) was selected for the *in vitro* system. Next, the effect of complete blockage of the IFN signaling pathway on virus replication was

investigated using ruxolitinib (**Fig. 1**). Enhanced A/mallard/NY/78-replication was observed in both A549 cells and Calu-3 cells when cells were treated with ruxolitinib, with larger enhancement of virus replication in A549 cells. After, blockage of the type I and/or the type III IFN signaling pathways by anti-IFNAR and/or anti-IFNLR Abs, respectively (**Fig. 1**), did not result in consistent enhancement of A/mallard/NY/78-replication. Lastly, Abs neutralizing individual IFNs were characterized using a luciferase reporter-based neutralization assay. These anti-IFN Abs can be used for follow-up experiments, in which the effect of blocking individual IFN on virus replication using these anti-IFN Abs will be assessed (**Fig. 1**). Besides the *in vitro* study of the effect of inhibition of the IFN system on IAV replication, this report includes the description of two side-projects. The first involved the cloning and production of a patient-derived anti-IFNα auto-Ab, which specifically targets all IFNα proteins with high affinity (*30*). This anti-IFNα Ab was included in the luciferase reported-based screen for neutralizing anti-IFN Abs. Clustered Regularly Interspaced Short Palindromic Repeats (CRISPR)/Cas9 mediated-knockout of type I IFNs (*IFNα*, *IFNß*, *IFNε*, *IFNκ*, and *IFNω*) and the *IFNAR1* and *IFNLR1* was the goal of the second side-project. At least 2 single cell clones with a knockout of *IFNε*, *IFNκ*, *IFNω*, *IFNAR1*, and *IFNLR1* were obtained. Knockout of all 13 *IFNα* genes was more complicated and is therefore still work in progress. For the CRISPR/Cas9-mediated knockout of *IFNß*, no knockout clones were obtained yet and a new guide RNA (gRNA) is needed. The next-generation sequencing (NGS), functional and western blot data of tested *IFNAR1* and *IFNLR1* single cell showed inconsistencies. Nevertheless, 2 *IFNAR1* and 3 *IFNLR1* single cell knockout clones were inoculated with A/mallard/NY/78, vesicular stomatitis virus (VSV)-GFP and parainfluenza virus 5 (PIV5)-GFP. No enhancement of A/mallard/NY/78-replication was observed in any of the *IFNAR1* and *IFNLR1* single cell knockout clones. Conversely, enhancement of PIV5-GFP and/or VSV-GFP-replication was observed in some *IFNAR1* and *IFNLR1* single cell knockout clones, however this was likely the result of clonal variability. Overall, further optimization is needed before the set-up assays and *in vitro* model system can be used to elucidate the molecular characteristics of anti-IFN auto-Abs and their relationship to virus replication.

Materials & Methods

Cells, IFNs, Abs, and ruxolitinib

A549 cells (ATCC; CCL-185), A549 2D8 cells (highly IFN-sensitive A549 sub-clone, described in Börold *et al*. (*31*)), 293T cells (ATCC; CRL-3216), MDCK cells (ATCC; NBL-2), and all derivates were maintained in Dulbecco's modified Eagle's medium (DMEM; Gibco), supplemented with 10% fetal bovine serum (FBS; Gibco), and 100 U/mL penicillin-streptomycin (Gibco) at 37 °C and 5% CO_2. Calu-3 cells (ATCC; HTB-55) were cultured in DMEM, supplemented with 20% FBS, and 100 U/mL penicillin-streptomycin. Ruxolitinib (Santa Cruz Biotechnology, sc-364729), IFNα2 (Novusbio, NPB2-34971), IFNß1b (pbl assay science, 11420-1), IFNω (Novusbio, NBP2-35893) IFNλ1 (Novusbio, NBP2-34996), and Abs against IFNAR1 (Abcam, ab124764), IFNAR2 (pbl assay science, 21385-1), IFNLR1 (pbl assay science, 21885-1), IFNα2 (Novusbio NB100-2479 (ST29)), IFNω (Novusbio, NBP2-99256), and IFNß (pbl assay science, 21465-1 (MMHB-15); pbl assay science, 21400-1 (MMHB-3); pbl assay science, 31410-1 (PAb)) were used according to the indicated concentrations.

Viruses, infections, and plaque assay

A/mallard/NY/6750/1978 (H2N2) IAV was provided by Silke Stertz, University of Zurich, Switzerland. A/mallard/NY/6750/1978 IAV was grown in eggs, ultracentrifuged, and stored in PBS. Viral titer was determined by plaque assay using MDCK cells as described below. PIV5-GFP was provided by Gauthier Lieber. PIV5-GFP was grown in Vero E6 cells, and viral titer was determined using Vero-CCL-81 cells. VSV-GFP was provided by Samira Schiefer. VSV-GFP was grown in Vero E6 cells, and viral titer was determined using Vero E6 cells. For infections with A/mallard/NY/6750/1978, 3E5 or 1.5E5 cells were seeded in 12-well plates or 24-well plates, respectively. Twenty-four hours after seeding, cells were inoculated with virus with the indicated MOI in phosphate-buffered saline (PBS; Gibco)-infection medium (PBSi), containing PBS, 0.3% bovine albumin, 100 U/mL penicillin-streptomycin, and 1 mM Ca^{2+}/Mg^{2+}. Inoculated cells were placed in the incubator for one hour at 37 °C and 5% CO_2, and were rocked every fifteen minutes to prevent drying out of the cells. The inoculum was removed and cells were washed three times with PBS before DMEM post-infection medium (DMEM, 100 U/mL penicillin-streptomycin, 0.3% bovine albumin, 0.1% FBS, and 20 mM Hepes) with 1 µg/mL TPCK trypsin was added, either with or without inhibitors or Abs, as indicated. Supernatant was harvested 1, 16, 24, 48, 72 and/or 96 hours after inoculation and stored at -80 °C. Virus titer in the harvested supernatant was quantified by an agarose plaque assay. For this procedure, MDCK were seeded to 100% confluency in 12-well plates. The next day, cells were washed with serum-free DMEM, supernatant from virus-infected cell cultures was serially diluted in PBSi, and used to inoculate confluent MDCK cells. One hour after incubating at 37 °C and 5% CO_2 (plates were rocked every fifteen minutes), the inoculum was removed and replaced by a standard agarose overlay (2x minimum essential medium (MEM) (70% H_2O, 20% 10x MEM, 4 mM glutamine, 200 U/mL penicillin-streptomycin, 0.3% $NaHCO_3$, 20 mM Hepes, 0.42% bovine serum albumin (BSA)), H_2O, 0.6% Oxoid agar, 0.1% $NaHCO_3$, 0.01% dextran DEAE, 0.01% TPCK trypsin). Inoculated cells were incubated at 37 °C and 5% CO_2 for 48 hours. Cells were fixed by adding formaldehyde saline on top for about 15 minutes before the agar overlay was removed. Fixed cells were subsequently stained with crystal violet for about 10 minutes and washed using running tap water. Plaques were counted by eye, and the titer, expressed as plaque forming units (PFU)/mL, was determined based on the number of plaques, dilution factor and inoculum volume.

RT-qPCR

Cells were lysed using BL + TG buffer (Promega), and cellular RNA was extracted using ReliaPrep RNA Cell Miniprep System (Promega), according to the manufacturer's instructions. Extracted RNA was converted into cDNA using the oligo(dT)15 primer (Promega) and a PCR nucleotide mix (Roche), which was followed by adding 5x first-strand buffer (Invitrogen), 0.1 M DTT (Invitrogen), RNasin ribonuclease

inhibitor (Promega) and SuperScript IV RT (Promega). PowerTrack SYBR Green (Applied Biosystems) was used in combination with primers for *18S* (primer sequences can be found in **Tab. S1**), *Actin*, *IFI44*, *ISG56*, *MX1*, *RSAD2*, *IFNα2, IFNß*, *IFNε*, *IFNκ*, *IFNω*, *IFNλ1*, or *IFNλ2/3*. RNA quantification was performed on a 7300 Real-Time PCR system (Applied Biosystems). The delta-delta-cycle of threshold (ΔΔCt) value was determined relative to the per experiment indicated control (*32*).

In-Fusion cloning

The used protocol and most consumables used for the In-Fusion cloning were obtained from Peter Rusert and Cyrille Niklaus, University of Zurich, Switzerland. The sequences for both the heavy (sequences can be found in **Tab. S2**) and the light chain of the anti-IFNα Ab were obtained from Meyer *et al*. (sequences were obtained from a patient-derived anti-IFNα auto-Ab (19D11) (*30*)). DNA-strings containing these sequences were ordered from Twist bioscience. The ordered DNA string was added to an Eppendorf tube containing H_2O, In-Fusion Snap Assembly Master Mix enzyme premix (Takara Bio), and the IgGheavy-vector or IgGkappa-vector (both vectors were obtained from Peter Rusert) for the cloning of the Ab heavy chain or the light chain, respectively. After incubation for 15 minutes at 50 °C, all of the In-Fusion-prep solution was transformed into high-competent XL-10 Gold bacteria (Agilent), according to the manufacturer's instructions. The bacteria were plated and grown overnight on lysogeny-bouillon (LB) plates containing 100 µg/mL carbenicillin. Three colonies were picked and grown overnight in LB medium containing 100 µg/mL carbenicillin. The DNA from the colonies was isolated using the QIAprep Spin Miniprep kit (Qiagen), according to the manufacturer's instructions. Isolated DNA was Sanger sequenced by Microsynth. Plasmids containing the correct sequence were expanded and isolated using the QIAfilter Plasmid Maxi Kit (Qiagen), and the obtained plasmids were transfected into 293T cells using PEI MAX (Polysciences). In brief, 2.5E5 293T cells/well were seeded in a 6-well plate. The next day, a transfection mix containing DMEM (without additives), plasmids expressing the heavy chain and the light chain (1000 ng/chain) and PEI MAX were incubated for about 25 minutes at room temperature before the mixture was added dropwise to the 293T cells. Transfection efficiency was determined by using a V5-tag-GFP encoding vector (provided by Samira Schiefer), which was transfected according to the same protocol as the anti-IFNα Ab encoding plasmids. GFP readout was performed 48 hours post transfection using a Leica DFC7000 T microscope. Transfected cells were incubated for one week at 37 °C and 5% CO_2, before the supernatant was harvested and centrifuged at 500 *g* for 3 minutes. The supernatant containing the anti-IFNα Ab was stored at -80 °C before usage.

Luciferase reporter-based neutralization assay

Twenty-four thousand 293T cells were reverse-transfected, using FuGene HD (Promega), with a plasmid containing the firefly luciferase gene under control of the IFN-inducible mouse *Mx1* promotor, and a control plasmid expressing *Renilla* luciferase under control of a constitutively active promotor, as described in Busnadiego *et al.* (*15*). Cells were incubated at 37 °C and 5% CO_2 for 24 hours. Next, commercially available Abs or the in-house produced anti-IFNα auto-Ab were incubated with an equal volume of IFN, both at the indicated concentrations, for 1 hour at room temperature in a shaker. The medium of the reverse-transfected 293T was replaced by the IFN and Ab mix, and subsequently incubated for 24 hours at 37 °C and 5% CO_2. Luciferase expression was determined by the Dual-Luciferase Reporter Assay System (Promega) using the PerkinElmer EnVision 2104 Multilabel Reader, according to the manufacturer's instructions. Firefly luciferase values were normalized to the Renilla luciferase values, and these values were compared to DMEM-stimulated 293T cells, as indicated.

Luminex IFN detection kit

A custom Millipore Milliplex Human IFN Panel (HIFN-130K-06C) was ordered from Merck. The ordered customized IFN detection kit contained magnetic beads coated with detection antibodies against

several IFN cytokines (IFNα2, IFNß, IFNω, IFNλ1, IFNλ2, and IFNλ3). Supernatant from virus-infected cells was first UV-inactivated (15 minutes using a UV-light-lamp (540 nm); plaque assay was performed to confirm inactivation of virus), before IFNs were quantified using the Milliplex Human IFN Panel according to the manufacturer's instructions. The Median Fluorescent Intensity was measured using a Luminex FLEXMAP 3D system. Human IFN panel standards and quality control samples were run in parallel to the supernatant samples. The standards were used to make a standard curve, which was used for the absolute quantification of IFNs protein concentrations in the supernatant samples. Quality control samples were used to ensure the robustness of the human IFN panel. The standard curves were made using Microsoft Excel. Calculated negative protein levels were set at a value of 0 pg/mL.

CRISPR/Cas9

crRNA sequences for *IFNß* (all sequences can be found in **Tab. S3**), *IFNε*, *IFNκ*, *IFNω*, *IFNAR1*, and *IFNLR1* were pre-designed and ordered from IDT. The 13 *IFNα* genes (*IFNα1, IFNα2, IFNα4, IFNα5, IFNα6, IFNα7, IFNα8, IFNα10, IFNα13, IFNα14, IFNα16, IFNα17 and IFNα21*) were targeted by three self-designed crRNAs that cover all 13 *IFNα* genes. The crRNAs were incubated with diluted 10X Alt-R CRISPR/Cas9 tracrRNA, ATTO 550 (IDT, 1075934) to form the gRNA. Next, gRNA was incubated with Alt-R S.p. HiFi Cas9 Nuclease V3 (IDT, 1081060) to form the RNP complex. For CRISPR-mediated knockout of the IFNα genes, Alt-R S.p. Cas9 Nuclease V3 (IDT, 1081058) was used instead of the HiFI Cas9 Nuclease V3 that was used for the targeting of the other genes. The RNP complex, consisting of the gRNA and the Cas9 nuclease was reverse transfected into 4E4 A549 2D8 cells using RNAi Max (Invitrogen). Forty-eight hours later, the cells were split into two wells. One well was used for next-generation sequencing of the targeted locus, and the other part was used for growing up the RNP-transfected cells. The expanded cells were used for single cell seeding. For this, cells were counted and diluted to a concentration of 90, 30, 10, and 3.33 cells/mL. Next, 100 µL of each dilution was added to 48 to 144 wells of a 96-well plate. The plates were examined a few days later using a light microscope to identify wells containing single cell clones. These single cell clones were split into two wells. One well was used for next-generation sequencing of the targeted locus, and the cells in the other well were stored at -80 °C.

Next generation sequencing

The genomic DNA of RNP-transfected A549 2D8 cells was harvested using the QuickExtract DNA Extraction SoIn 1.0 (Lucigen), according to the manufacturer's instructions. Harvested genomic DNA was amplified using the KAPA HiFi HotStart ReadyMix (Roche), according to the manufacturer's instructions. The used primers were ordered at Microsynth (sequences can be found in **Tab. S3**). After mixing, amplification of the isolated DNA was performed using either a Bio-Rad T100 thermal cycler or a Biometra T3 thermocycler with the following protocol: 5 minutes at 98 °C, 18 cycles of 20 seconds at 98 °C, 15 seconds at 58 °C and 1 minute at 72 °C, followed by 2 minutes at 72 °C, and cooled down and stored at 4 °C. Next, a second polymerase chain reaction (PCR) run was performed to ligate barcodes to the amplified genomic DNA. For this, the KAPA HiFi HotStart ReadyMix was again used according to the manufacturer's instructions. The PCR program used for barcode ligation consisted of 5 minutes at 98 °C, 18 cycles of 20 seconds at 98 °C, 15 seconds at 60 °C and 1 minute at 72 °C, followed by 2 minutes at 72 °C, and cooled down and stored at 4 °C. Samples were pooled, and the DNA was extracted using the Wizard SV Gel and PCR Clean-Up System (Promega), according to the manufacturer's instructions. The DNA concentration was measured using a NanoDrop ND-1000 spectrophotometer and diluted to a final concentration of 4 nM. The pooled diluted sample was subjected to next generation sequenced (NGS) by the diagnostics department of the Institute of Medical Virology, University of Zurich, Switzerland using the Illumina MiSeq technology. The obtained sequence was compared to the human genome reference sequence using a script written by Davide Eletto. An insertion or deletion of nucleotides not dividable by 3 was considered a knockout.

Agarose gel electrophoresis

To check whether the PCR primers were able to amplify the harvested genomic DNA from the RNP-transfected A549 2D8 cells, PCR products were run on an agarose gel. For this, harvested DNA was amplified using the following protocol: 5 minutes at 98 °C, 30 cycles of 20 seconds at 98 °C, 15 seconds at 58 °C and 1 minute at 72 °C, followed by 2 minutes at 72 °C, and cooled down and stored at 4 °C. GelPilot Loading Dye (Qiagen) was added to the samples, before they were loaded onto a 2% agarose gel containing GelRed (Biotium). GeneRuler 100 bp DNA ladder Plus (Fermentas) was added in a separate lane as a marker. The gel was run at 100 V for about 75 minutes using a Bio-Rad PowerPac Basic power supply. The gel was imaged using a Vilber E-BOX. Results of the agarose gel electrophoresis are not shown.

Western blotting

Cells were harvested and lysed using urea disruption buffer (6 M urea, 4% SDS, 1 M β-mercaptoethanol, bromophenol blue). After transferring the cells to Eppendorf tubes, the samples were sonicated (Branson Digital Sonifier SFX 250) with 5 pulses for each sample. Lysed samples were loaded into pre-casted Bolt 4-12% bis-tri plus mini protein gels (Invitrogen), and run using a mini gel tank (Invitrogen) and a PowerPac power supply at 170 V, containing Bolt MOPS SDS running buffer. Precision Plus Protein™ All Blue Prestained Protein Standards (Bio-Rad) was used as a marker. Proteins were transferred from the gel to a nitrocellulose membrane using a mini blot module (Invitrogen) inside a mini gel tank containing Bolt transfer buffer (Invitrogen) plus 10% methanol at 15 V for 1 h. The nitrocellulose membrane was incubated in a blocking solution (10% milk (w/v) in PBS-Tween 0.1%) for 30 minutes at room temperature. Next, the membrane was stained for IFNAR1 or IFNLR1 using an Ab solution (1:1000, 1% milk in PBS-Tween 0.1%) overnight at 4 °C. The blot was washed 3 times in PBS-Tween 0.1%, and the membrane was stained with secondary Ab solution (1:5000, 1% milk in PBS-Tween 0.1%) for 1 hour at room temperature. The used secondary Abs were IRDye 800CW goat anti-mouse (LI-COR, 92632210) and IRDye 800CW goat anti-rabbit (LI-COR, 92632211). Blot was washed 3 times for 20 minutes at room temperature with PBS-Tween 0.1%, and the membrane was imaged using a LI-COR Odyssey Fc Imager. Images were analyzed using Image Studio Lite Ver. 5.2.

Incucyte live cell analysis

Twenty-four thousand cells (A549 2D8 cells and *IFNAR1* and *IFNLR1* knockout clones) were seeded in a 96-wells plate 24 hours prior to inoculation. Cells were inoculated with either PIV5-GFP or VSV-GFP with a range of MOIs, ranging from 10 to 0.0001. For infection with PIV5-GFP, cells were inoculated in PBSi for 1 hour. The plate was rocked every 15 minutes to ensure equal virus distribution. Inoculum was removed, cells were washed 3 times with PBS before post-infection medium containing 1 µg/mL TPCK trypsin and 5 µM ruxolitinib or DMSO was added. For infection with VSV-GFP, cells were inoculated with virus-containing post-infection medium, which included 5 µM ruxolitinib or DMSO. The inoculated cells were placed into the Sartorius Incucyte S3 Live Cell Analysis Instrument, which was located inside a cell culture incubator set at 37 °C and 5% CO_2. Two images per well were taken every 3 hours, starting 1 h.p.i. for VSV-GFP-infected cells and 2 h.p.i. for PIV5-GFP-infected cells. A magnification of 10x was used to image cell confluency and measure the GFP signal. Analysis of the images was performed using the Incucyte 2022B Rev2 software (Sartorius). Cell confluency was determined using the AI Confluence setting, without additional filters. Green area was determined using the Top-Hat setting, with a radius of 10 µM and a Green calibrated Unit (GCU) threshold of 0.2 for PIV5-GF-infected cells and 0.5 for VSV-GFP-infected cells. For every image, the area that was positive for GFP was divided by the area that was covered by cells, and this percentage was used as a proxy for the percentage of infected cells.

Figures and statistical analysis

Figures were made using GraphPad Prism v10. Statistical analysis was performed using GraphPad Prism v10. Data were analyzed using a Kruskal-Wallis Test followed by Dunn's Test for multiple comparison. For **Fig. 10b-e**, first the area under the curve (AUC) was calculated for each replicate before a Kruskal-Wallis Test followed by Dunn's Test was performed. The AUC in **Fig. 10b** was calculated from T=32-98 h.p.i., in **Fig. 10c** from T=38h-98 h.p.i., in **Fig. 10d** from 10-37 h.p.i., and in **Fig. 10e** from 13-49 h.p.i., which was based on when an initial increase in Green Area (%) was observed. *P* values less than 0.05 were considered significant. * = *P* value ≤ 0.05, ** = *P* value ≤ 0.01.

Results

Effect of ruxolitinib on A/mallard/NY/78-replication in Calu-3 and A549 cells

In an initial screen, A549 cells were inoculated with different IAVs in the presence of ruxolitinib or DMSO to determine the effect of ruxolitinib on viral replication over time (results not shown). Ruxolitinib is a JAK inhibitor, and the addition of ruxolitinib results in the inhibition of the IFN signaling pathway (*33–35*). With this screen, several IFN-sensitive IAVs were identified. One of the IAVs for which enhanced replication in the presence of ruxolitinib was observed was A/mallard/NY/78. A/mallard/NY/78 might therefore be a good model virus to study the effect of (partial) blockage of the IFN signaling pathway on viral replication. To confirm the observed enhanced A/mallard/NY/78-replication upon treatment with ruxolitinib and to select a model cell line, follow-up experiments were performed to establish an initial *in vitro* model system for the study of anti-IFN auto-Abs.

In the initial screen, A549 cells were used to identify IFN-sensitive IAVs. After A/mallard/NY/78 was identified as an IFN-sensitive virus, it was tested whether enhanced A/mallard/NY/78-replication could be observed in multiple cell lines, and in which cell line the ruxolitinib-mediated enhancement of A/mallard/NY/78-replication would be the largest. However, before cells were inoculated with A/mallard/NY/78 in the presence of ruxolitinib, a reverse transcriptase-quantitative PCR (RT-qPCR) of expressed ISGs by IFN-stimulated A549 or Calu-3 cells in the presence or absence of ruxolitinib was performed (**Fig. 2a-b**). Calu-3 (**Fig. 2a**) or A549 (**Fig. 2b**) cells were seeded for 56 or 40 hours, respectively, before 1000 IU/mL IFNα2 and/or 5 µM ruxolitinib was added for 8 hours (Calu-3 cells) or 16 hours (A549 cells). These timepoints were chosen as supernatant of inoculated cells would be harvested for virus titration up to 72 hours post infection (h.p.i.). IFNα2 stimulation increased ISG expression levels for all selected ISGs in both Calu-3 and A549 cells. Treatment of 5 µM ruxolitinib prior to IFNα2 stimulation did not result in increased ISG expression levels in both A549 and Calu-3 cells, indicating that 5 µM ruxolitinib completely blocked IFN signaling. Besides, treatment of cells with 5 µM ruxolitinib alone resulted in reduced ISG expression levels, suggesting that ruxolitinib can inhibit tonic IFN signaling in both A549 cells and Calu-3 cells. Based on this experiment it was decided to continue with a concentration of 5 µM ruxolitinib to block complete IFN signaling in A549 and Calu-3 cells.

Next, it was tested whether the addition of 5 µM ruxolitinib enhanced A/mallard/NY/78-replication in A549 and Calu-3 cells. Calu-3 and A549 cells were inoculated with A/mallard/NY/78 in the presence of 5 µM ruxolitinib or DMSO (ruxolitinib or DMSO was added 1 h.p.i.) (**Fig. 3a-h**). Cells were inoculated with a range of MOIs (0.03, 0.01, 0.003, and 0.001) to identify a MOI at which enhancement of viral replication would be the largest. In both Calu-3 and in A549 cells, there was an enhancement of A/mallard/NY/78-replication when cells were treated with ruxolitinib. This enhancement of virus replication was observed for all used MOIs, with the largest enhancement observed at 48 h.p.i. when a MOI of 0.003 was used to inoculate Calu-3 cells (**Fig. 3c**) and a MOI of 0.001 for A549 cells (**Fig. 3h**). For most used MOIs, enhancement of A/mallard/NY-replication was already observed at 24 h.p.i., increased enhancement of virus replication was seen at 48 h.p.i. for all conditions, and continued enhancement of A/mallard/NY/78-replication at 72 h.p.i. was observed for most conditions. In Calu-3 cells, treatment with ruxolitinib resulted in a 3-10-fold enhancement in viral titers at 48 h.p.i., and a 0-3-fold enhancement at 72 h.p.i. (**Fig. 3a-d**). For A549 cells, the treatment with ruxolitinib enhanced viral titers around 10-fold for all MOIs at 48 h.p.i., and at 72 h.p.i. there was a 3-100-fold enhancement in viral titers (**Fig. 3e-h**). Based on these results it was decided to continue with A549 cells and use this human lung tissue cell line for the model system to study anti-IFN auto-Abs *in vitro*, as ruxolitinib-mediated enhancement of A/mallard/NY/78-replication was larger in A549 cells than in Calu-3 cells.

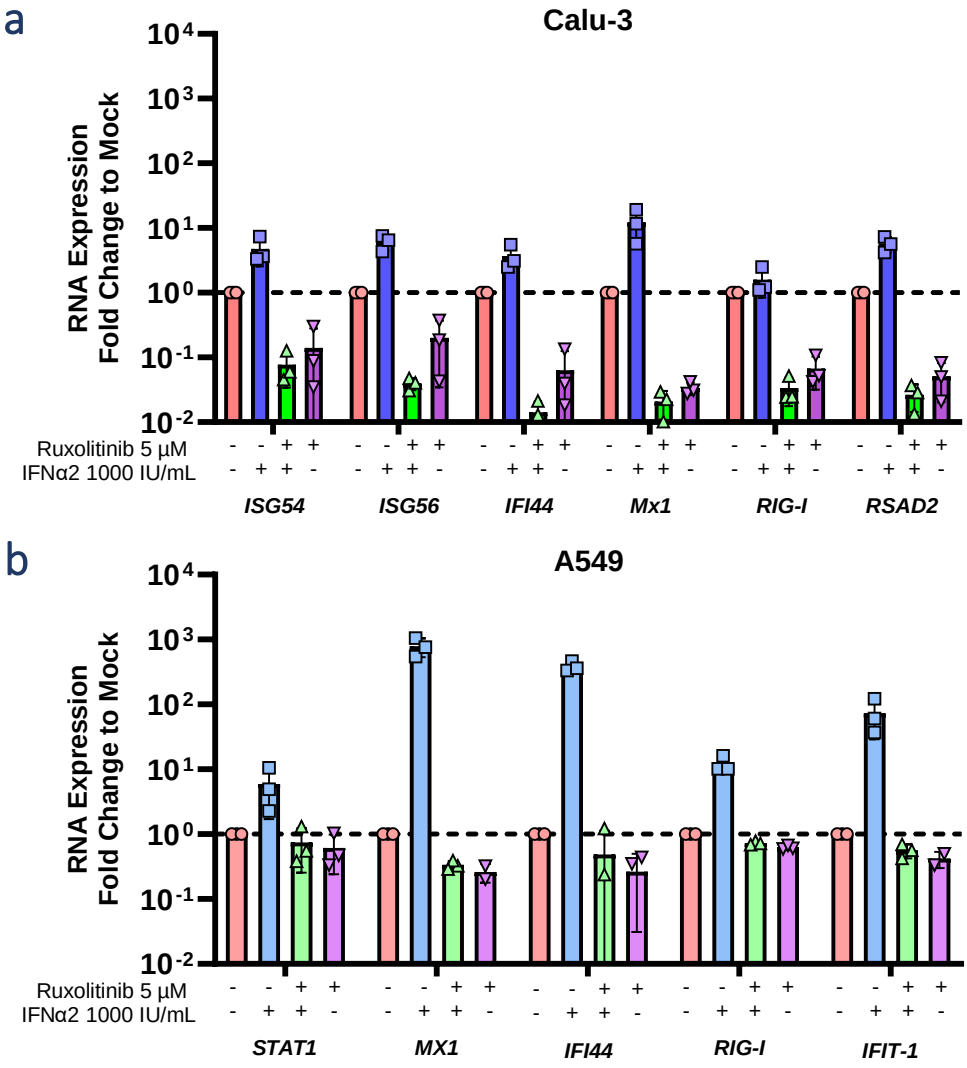

Fig. 2a-b. Effect of ruxolitinib-treatment on tonic and IFNα2-induced ISG expression levels in Calu-3 cells and A549 cells. a) Calu-3 cells were treated with 5 µM ruxolitinib or DMSO for 40 hours and stimulated with 1000 IU/mL IFNα2 or a similar volume of PBS in DMEM for 8 hours. Cells were harvested, RNA was isolated, and ISG expression levels were quantified by RT-qPCR. Values were normalized to unstimulated DMSO-treated Calu-3 cells. **b)** A549 cells were treated with 5 µM ruxolitinib or DMSO for 56 hours and stimulated with 1000 IU/mL IFNα2 or a similar volume of PBS in DMEM for 16 hours. Cells were harvested, RNA was isolated, and ISG expression levels were quantified by RT-qPCR. Values were normalized to unstimulated DMSO-treated A549 cells.

After it was determined which model virus and cell line would be used for the *in vitro* system, the inoculation experiments were repeated in triplicate to establish which MOI would be used for follow-up experiments. Two MOIs (0.03 and 0.003) were chosen based on their pronounced growth curves in the previous experiment (**Fig. 3e, g**). Similar to the previous experiment, enhancement of A/mallard/NY/78-replication was observed at 24 h.p.i., increased enhancement of virus replication was seen at 48 h.p.i, and this enhancement of A/mallard/NY/78-replication continued to increase at 72 h.p.i. for both MOIs (**Fig. 3i-j**). The observed enhancement of virus replication was larger at all timepoints when a MOI of 0.03 was used (**Fig. 3i**) compared to when a MOI of 0.003 was used (**Fig. 3j**). Therefore, it was decided that a MOI of 0.03 would be used for the *in vitro* model system. Thus, after the initial experiments in which the effect of ruxolitinib on ISG expression levels and A/mallard/NY/78-replication in Calu-3 and A549 cells was observed, the *in vitro* system for the study of anti-IFN auto-Abs was established, consisting of A549 cells and A/mallard/NY/78 with a MOI of 0.03.

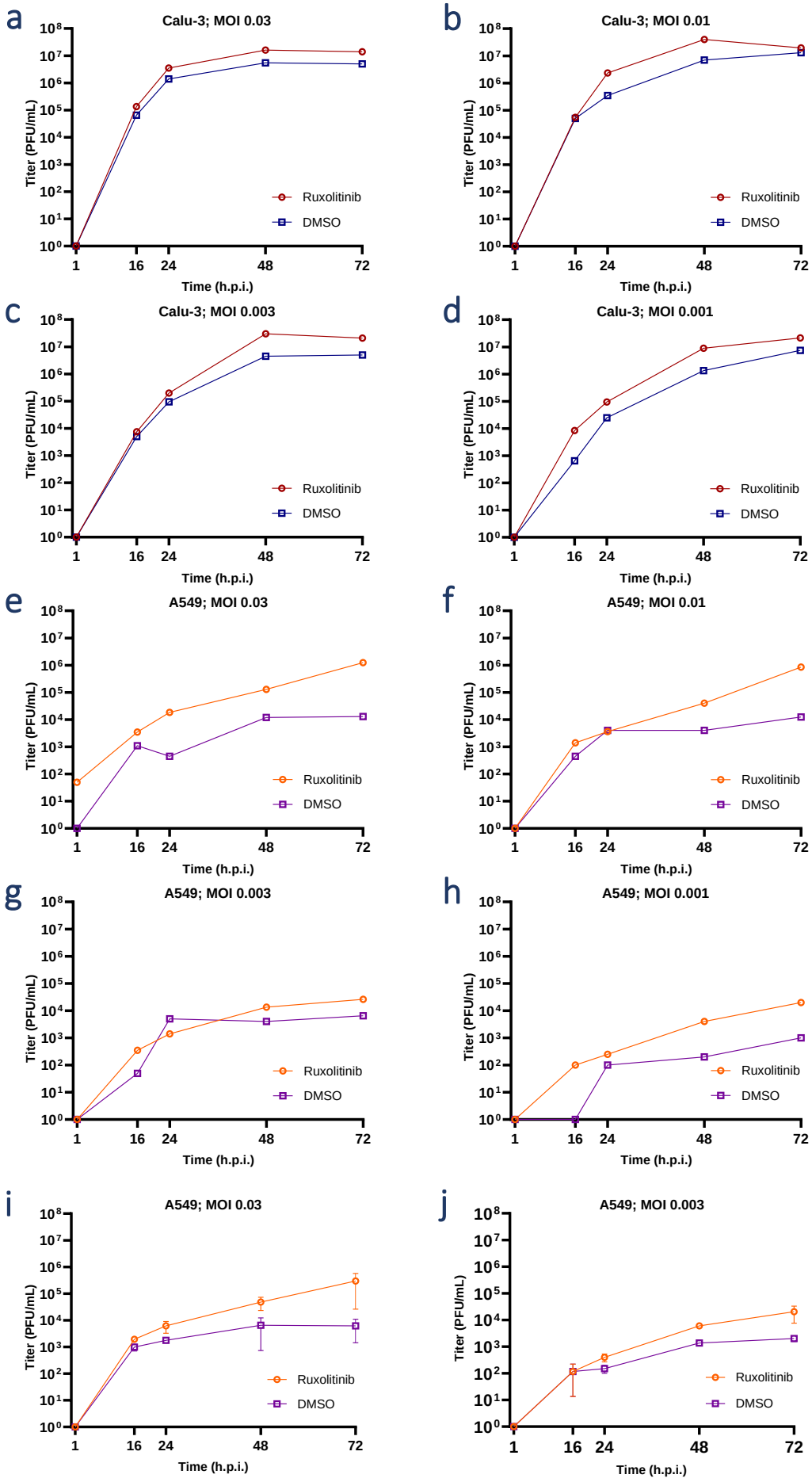
a
Calu-3; MOI 0.03
b
Calu-3; MOI 0.01
c
Calu-3; MOI 0.003
d
Calu-3; MOI 0.001
e
A549; MOI 0.03
f
A549; MOI 0.01
g
A549; MOI 0.003
h
A549; MOI 0.001
i
A549; MOI 0.03
j
A549; MOI 0.003
Titer (PFU/mL)
Time (h.p.i.)
Ruxolitinib
DMSO

Fig. 3a-j. Replication kinetics of A/mallard/NY/78 in ruxolitinib- or DMSO-treated Calu-3 cells and A549 cells. a-d) Calu-3 cells were inoculated with A/mallard/NY/78 with a MOI of 0.03 (**a**), 0.01 (**b**), 0.003 (**c**), or 0.001 (**d**). Cells were treated with ruxolitinib or DMSO 1 h.p.i., and supernatant was harvested over time. Virus titers in the harvested supernatants were quantified by plaque assay. **e-h)** A549 cells were inoculated with A/mallard/NY/78 with a MOI of 0.03 (**e**), 0.01 (**f**), 0.003 (**g**), or 0.001 (**h**). Cells were treated with ruxolitinib or DMSO 1 h.p.i., and supernatant was harvested over time. Virus titers in the harvested supernatants were quantified by plaque assay. **i-j)** A549 cells were inoculated with A/mallard/NY/78 with a MOI of 0.03 (**i**) or 0.003 (**j**) in triplicate. Cells were treated with ruxolitinib or DMSO 1 h.p.i., and supernatant was harvested over time. Virus titers in the harvested supernatants were quantified by plaque assay.

Effect of anti-IFNAR and/or anti-IFNLR Abs on A/mallard/NY/78-replication in A549 cells

Next, the effect of blocking type I and/or type III signaling on A/mallard/NY/78-replication in A549 cells was assessed by neutralizing the IFNAR and/or the IFNLR using commercially available Abs. By blocking the type I IFN receptor (IFNAR) or the type III IFN receptor (IFNLR) it would be possible to determine the contribution of type I IFN and type III signaling on the inhibition of A/mallard/NY/78-replication in A549 cells. First, to get an idea which IFNs were expressed by A549 upon A/mallard/NY/78-infection and at what level, an experiment was performed in which A549 cells were inoculated with A/mallard/NY/78 with a MOI of 0.03, which was followed by a RT-qPCR of type I and type III IFNs (**Fig. 4a-g**). Cells were harvested over time at the same timepoints as taken for viral replication curves. The mRNA expression levels were normalized to mRNA expression levels of mock-infected cells from the same timepoint. For the type I IFNs *IFNα2* and *IFNß* there was an increase in mRNA expression levels over time, with a peak of mRNA expression levels at 48 h.p.i. (**Fig. 4a-b**). In contrast, the mRNA expression levels of the other type I IFNs included (*IFNε, IFNκ,* and *IFNω*) did not increase (**Fig. 4c-e**). mRNA expression levels of type III IFNs, *IFNλ1* and *IFNλ2/3* increased over time, and the peak of mRNA expression levels was observed at 48 h.p.i. for both type III IFN genes (**Fig. 4f-g**).

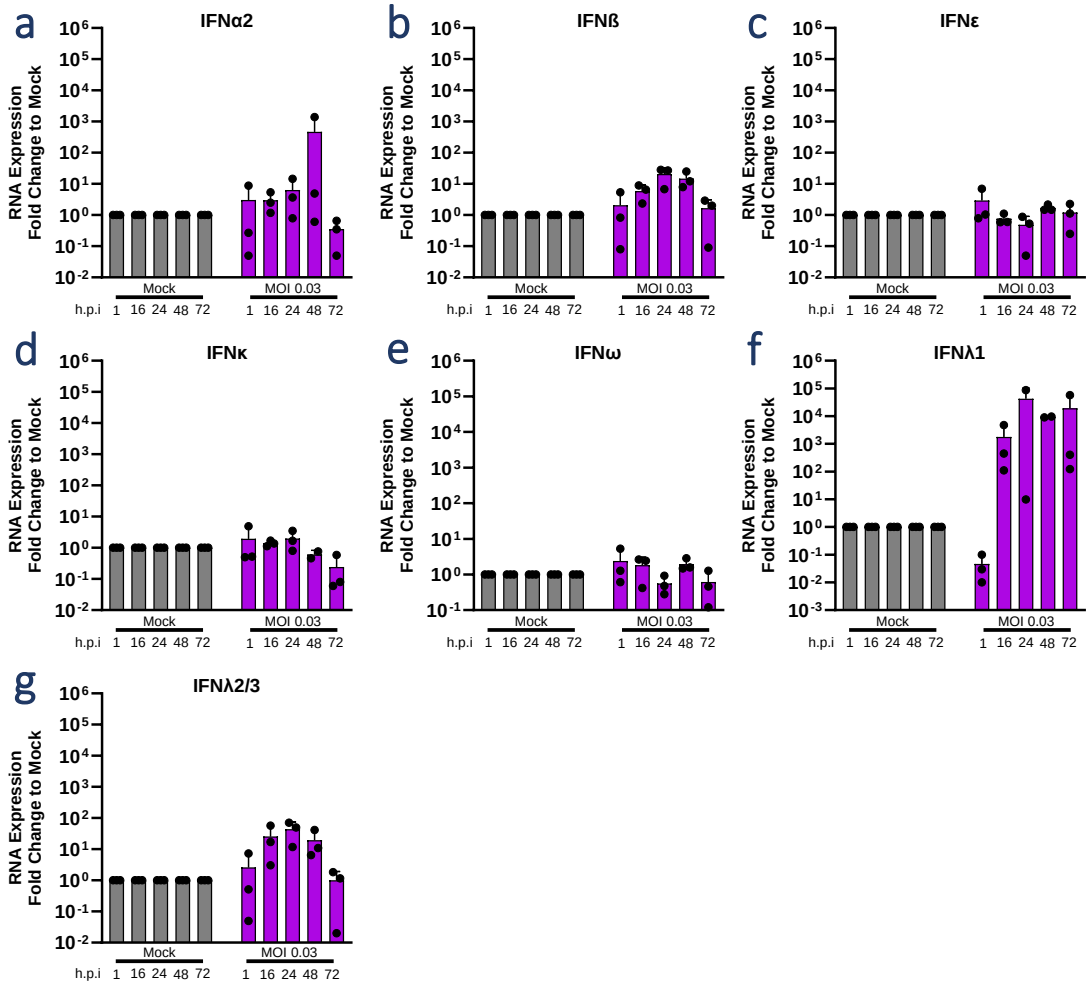

Fig. 4a-g. mRNA expression levels of *IFNα2*, *IFNß*, *IFNλ1*, and *IFNλ2/3* upon A/mallard/NY/78-infection in A549 cells. a-g) A549 cells were inoculated with A/mallard/NY/78 with a MOI of 0.03. Mock-infected A549 cells were included as a control. Cells were harvested over time, RNA was isolated, and *IFNα2* (**a**), *IFNß* (**b**), *IFNε* (**c**), *IFNκ* (**d**), *IFNω* (**e**), *IFNλ1* (**f**), and *IFNλ2/3* (**g**) mRNA expression levels were quantified by RT-qPCR. Values were normalized to mock-infected A549 cells per timepoint.

The RT-qPCR experiment showed which IFNs were expressed over time by A549 cells upon A/mallard/NY/78-infection, but it did not provide information about IFN protein levels. The method used to determine what levels of IFNs needed to be blocked by the commercial IFNAR and IFNLR Abs involved the comparison between ISG expression levels by A549 cells upon A/mallard/NY/78-infection and ISG expression levels by A549 cells upon stimulation with individual IFNs. The comparison between both ISG expression levels was used as a substitute for directly measuring IFN protein levels. The cells used in **Fig. 4a-g** (for the quantification of mRNA expression levels of IFNs) were also used to quantify ISG expression levels by A/mallard/NY/78-infected A549 cells. Besides, a range of concentrations of IFNα2, IFNλ1, IFNß, and IFNω was used for the stimulation of A549 cells. A RT-qPCR was performed for three different ISGs: *IFI44*, *ISG56* and *MX1* (**Fig. 5a-c**). The pattern of mRNA expression levels of all three ISGs was comparable, as the expression levels of peaked at 48 h.p.i. (the peak of *IFI44* expression levels at 72 h.p.i. was the result of one extreme high value). For *MX1* expression levels, also an earlier peak at 16 h.p.i. was observed (**Fig. 5c**). The RT-qPCR data of IFN-stimulated A549 cells showed that lower ISG expression levels were observed when a lower amount of IFN was used, as expected (**Fig. 5a-c**). The comparison of ISG expression levels in A/mallard/NY/78-infected A549 cells at 48 h.p.i. with the IFN-stimulated A549 cells showed that ISG expression levels in virus-infected A549 cells were comparable to ISG expression levels of A549 cells stimulated with 3-10 IU/mL IFNα2, 10-30 IU/mL IFNλ1, 1-10 IU/mL IFNß, or <1-10 IU/mL IFNω (**Fig. 5a-c**). Based on these results it was concluded that the anti-IFNAR Ab needed to block at least 10 IU/mL of type I IFN-stimulation and anti-IFNLR Abs needed to block at least 30 IU/mL of type III IFN-stimulation. Initially it was tried to block 30 IU/mL of either type I or type III IFN using the commercial anti-IFNAR or anti-IFNLR Abs, respectively. Later, it was attempted to neutralize 100 IU/mL.

Besides, the other method used to determine IFN protein levels produced by A549 cells upon infection with A/mallard/NY/78 was the Luminex IFN detection kit. Quantification of IFN protein levels by this IFN kit was only performed towards the end of the project as it took months before the IFN kit arrived. The results of the assay used to quantify IFN protein levels over time can be found in the supplementary materials (**Fig. S1a-f**). In short, the IFN detection kit results were in line with the RT-qPCR data of A/mallard/NY/78-infected A549 cells (**Fig. 4a-g**) as there was mainly type III IFN production and no increase in production of type I IFNs upon infection with A/mallard/NY/78.

After assessing how many IU/mL of type I IFN or type III IFN the anti-IFNAR or the anti-IFNLR Ab needed to block, respectively, it was determined what concentrations of Abs were needed to block 30 IU/mL of type I IFN or type III IFN. First, anti-IFNAR2 Ab or anti-IFNLR1 Ab were added to A549 cells with increasing concentration. After pre-incubation, 30 IU/mL of IFNα2 or IFNλ1 was added to the supernatant and cells were incubated for 16 hours. Cells were harvested, RNA was isolated, and ISG expression levels were quantified by RT-qPCR. ISG expression levels were normalized to mock-treated control (**Fig. 6a-c**). Stimulation of A549 cells with IFNα2 or IFNλ1 in the absence of the anti-IFNAR Ab or anti-IFNLR Ab resulted in increased ISG expression for all three included ISGs. The addition of the anti-IFNAR Ab with a concentration of 0.3 and 1 µg/mL almost completely blocked the induction of ISG expression, whereas for the anti-IFNLR1 Ab an effect was observed with a concentration of 1 µg/mL only. The used Ab concentrations did not completely inhibit ISG expression levels upon stimulation with either IFNα2 or IFNλ1, but the reductions with a concentration of 0.3 µg/mL for the anti-IFNAR2 Ab and 1 µg/mL for the anti-IFNLR1 Ab were adequate, and these concentrations were chosen for the follow-up inoculation experiment.

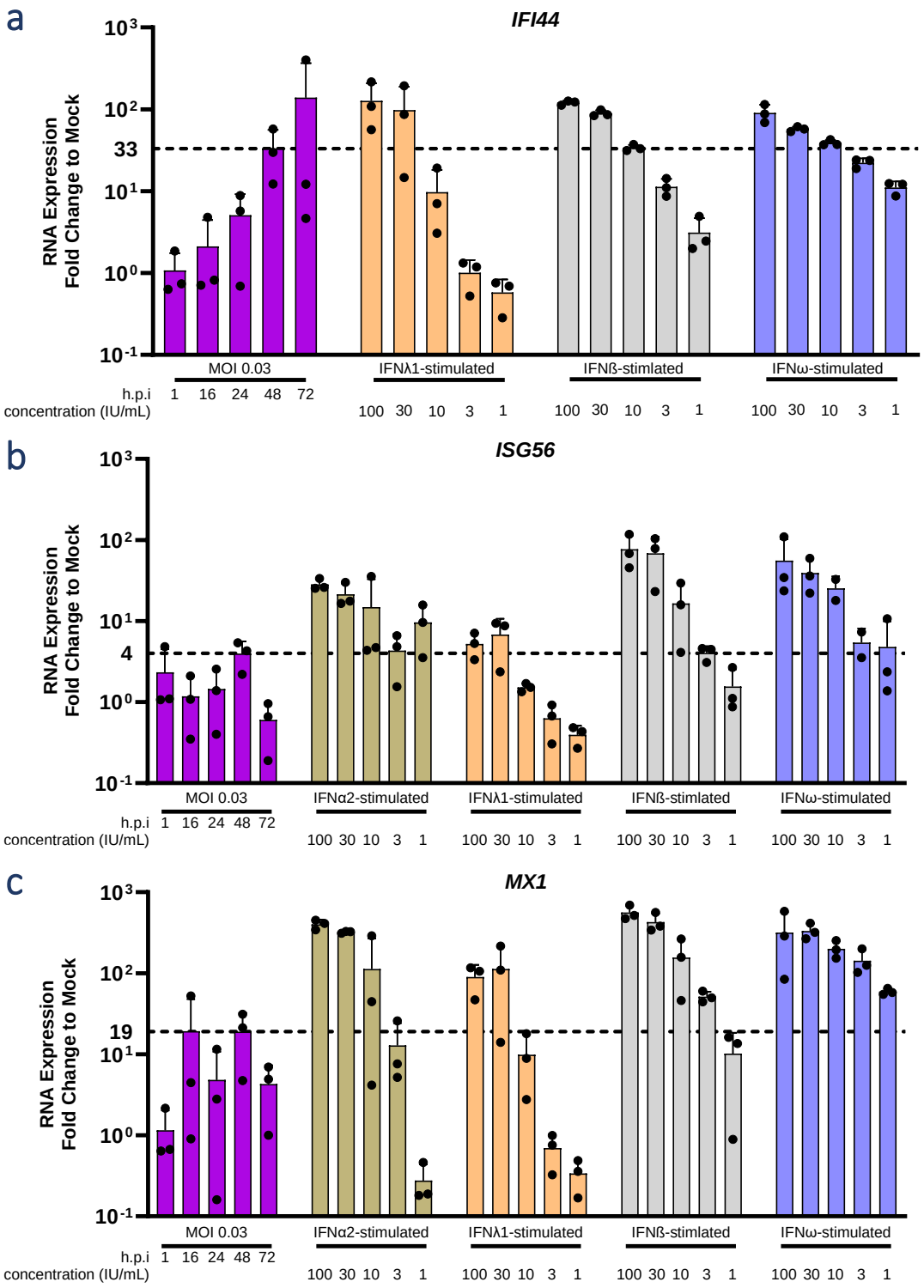

Fig. 5a-c. ISG expression levels of A/mallard/NY/78-infected A549 cells and IFN-stimulated A549 cells. a-c) A549 cells were inoculated with A/mallard/NY/78 with a MOI of 0.03. Mock-infected A549 cells were included as a control. Cells were harvested over time, RNA was isolated, and *ISG56* (**a**), *MX1* (**b**), and *IFI44* (**c**) mRNA expression levels were quantified by RT-qPCR. Values were normalized to mock-infected A549 cells per timepoint. A549 cells stimulated with a concentration range of *IFNα2* for 8 hours or *IFNλ1*, *IFNß*, or *IFNω* for 16 hours were taken along as control. Cells were harvested, RNA was isolated and *ISG56* (**a**), *MX1* (**b**), and *IFI44* (**c**) mRNA expression levels were quantified by RT-qPCR. Values were normalized to unstimulated A549 cells.

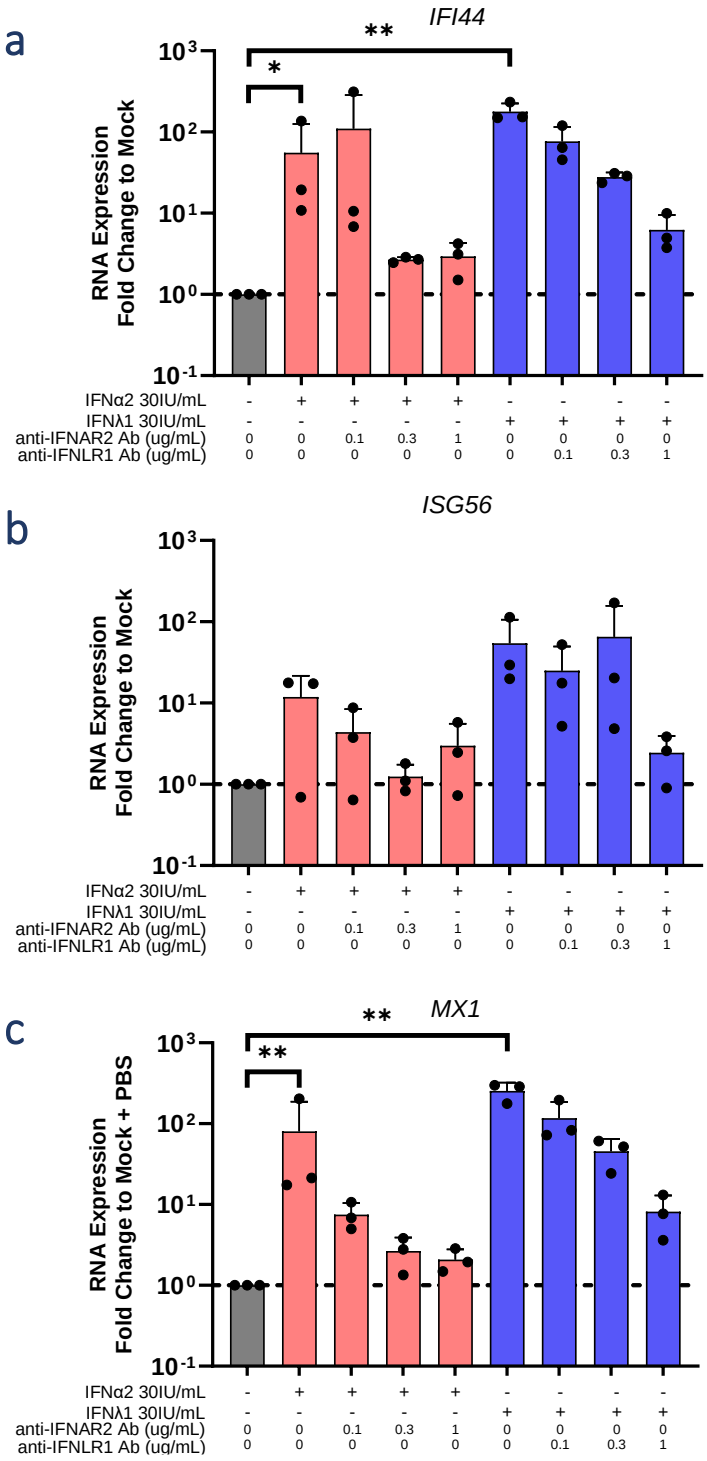

Fig. 6a-c. Inhibition of IFNα2- and IFNλ1-induced ISG expression levels by anti-IFNAR and anti-IFNLR Abs. a-c) A549 cells were treated with anti-IFNAR or anti-IFNLR Abs for 24 hours and stimulated with 30 IU/mL IFNα2, IFNλ1, or a similar volume of PBS in DMEM for 16 hours. Cells were harvested, RNA was isolated, and *IFI44* (**a**), *ISG56* (**b**), and *MX1* (**c**) mRNA expression levels were quantified by RT-qPCR. Values were normalized to unstimulated PBS-treated A549 cells.

To determine the inhibitory capacity of the anti-IFNAR2 and/or anti-IFNLR1 Abs on A/mallard/NY/78-replication, A549 cells were inoculated with a MOI of 0.03, and 1 h.p.i. post-infection medium containing anti-IFNAR2 Ab (0.3 µg/mL), anti-IFNLR1 Ab (1 µg/mL), both Abs, or PBS was added to the cells. Supernatant was harvested and titrated over time to determine the inhibitory effect of these anti-IFN-receptor Abs on multicycle virus replication in A549 cells. The presence of anti-IFNAR2 Ab resulted in enhanced replication of A/mallard/NY/78 in A549 compared to mock-treated infected cells

at 48 and 72 h.p.i. (**Fig. 7a**). Enhancement of replication was also observed at 48 h.p.i. when only the anti-IFNLR1 Ab was added. Treatment with both Abs at the same time did not result in enhancement of A/mallard/NY/78-replication. Since these results were contradictive, the experiment was repeated twice (**Fig. 7b-c**).

Before repeating the experiment, the amount of anti-IFNAR or anti-IFNLR Ab needed to neutralize 100 IU/mL IFNα or IFNλ1 was determined, respectively, instead of the 30 IU/mL used before. This was done to be sure that the used Abs would block all type I or type III IFN signaling throughout the course of infection. The experiment in **Fig. 6a-c** was repeated, with higher concentrations of IFNs and Abs (**Fig. S2a-f**). Complete inhibition of 100 IU/mL IFNλ1 stimulation by the anti-IFNLR1 Ab was obtained with a concentration of 1, 3, and 5 µg/mL, whereas the anti-IFNAR2 Ab was not able to completely inhibit IFNα2 stimulation. Nevertheless, an evident reduction in ISG expression was observed when a concentration of 20 µg/mL anti-IFNAR2 Ab was used, and this concentration was used to assess the effect of anti-IFNAR and/or anti-IFNLR Abs on A/mallard/NY/78-replication in A549 cells.

In the first experiment in which 0.3 µg/mL anti-IFNAR2 Ab and/or 1 µg/mL anti-IFNLR1 Abs were used, an effect of the addition was observed when either anti-IFNAR2 or anti-IFNRL Ab was added (**Fig. 7a**). The experiment was repeated with higher concentrations of added Abs. In the first repeat (**Fig. 7b**), a minor enhancement of A/mallard/NY/78-replication in A549 cells was observed at 48 h.p.i. when the anti-IFNAR2 Ab was added or when both Abs (anti-IFNAR2 Ab and anti-IFNLR1 Ab) were added. No enhancement was observed when only the anti-IFNLR1 Ab was added. For the second repeat, no enhancement of A/mallard/NY/78-replication was observed at all (**Fig. 7c**). Overall, the 3 replicates showed inconsistent results, and therefore no clear effect of the anti-INFAR2 Ab and the anti-IFNLR1 Ab on A/mallard/NY/78-replication in A549 cells was observed.

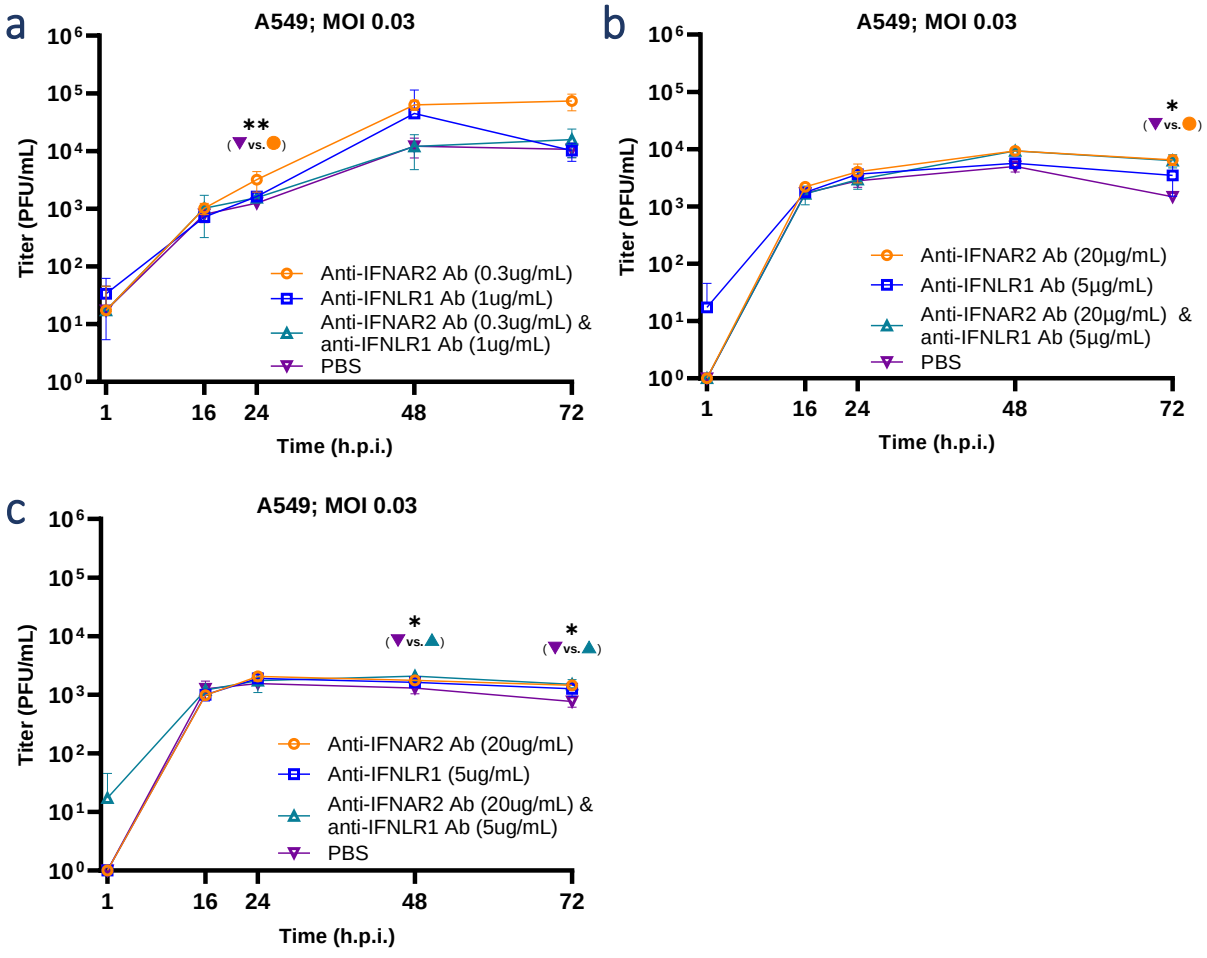

Fig. 7a-c. Replication kinetics of A/mallard/NY/78 in anti-IFNAR Ab- and/or anti-IFNLR Ab- or mock-treated A549 cells. a-c) A549 cells were inoculated with A/mallard/NY/78 with a MOI of 0.03. Cells were treated with anti-IFNAR Ab and/or anti-IFNLR Ab or an equivalent volume of PBS 1 h.p.i., and supernatant was harvested over time. Virus titers in the harvested supernatants were quantified by plaque assay.

Cloning and production of an anti-IFNα auto-Ab, and characterization of neutralizing anti-IFNα, anti-IFNß, and anti-IFNω Abs

Due to the timing of the performed experiments, assays were performed in parallel to characterize neutralizing anti-IFN Abs before it was observed that no consistent enhancement of A/mallard/NY/78-replication was observed when cells were treated with anti-IFNAR and/or anti-IFNLR Abs. In addition, if in the future a (influenza A) virus would be identified for which enhancement could be obtained when the type I and/or type III IFN system is blocked, it would speed-up follow-up research when neutralizing anti-IFN Abs would already be characterized. First, a side-project was devised, which involved the generation of an anti-IFNα Ab that neutralizes all 13 IFNα proteins. Meyer *et al*. described the characterization of an autoimmune regulator (AIRE)-deficient patient-derived neutralizing anti-IFNα-auto-Ab (19D11), which was cloned and produced here as part of the project (*30*). For the Ab In-Fusion Cloning, the protocol and most In-Fusion Cloning reagents were obtained from Peter Rusert and Cyrille Niklaus, University of Zürich, Switzerland. In short, sequences for the heavy chain and light chain were ordered cloned into a vector coding for an IgG heavy chain and an IgG kappa chain, respectively, using the In-Fusion Snap Assembly Master Mix, according to the manufacturer's protocol. Both cloned vectors were sequenced by Sanger sequencing to confirm the correct sequence. 293T cells were transfected with the vectors encoding the IgG heavy and kappa chain, or mock-transfected, and supernatants were harvested 7-days post-transfection.

After harvesting, the neutralization capacity was tested. The assay performed to test the neutralization capacity of the in-house-produced anti-IFNα Ab and of commercially available Abs was described in Busnadiego *et al*. (*15*), and is depicted in **Fig. 8a**. For this luciferase reporter-based neutralization assay, 293T cells were transfected with luciferase-based IFN-reporter constructs. Twenty-four hours after seeding, a pre-incubated mixture of type I or type III IFN with the in-house-produced anti-IFNα Ab or a commercial Ab was added to the 293T cells. Cells were incubated for 24 hours and IFN-stimulated luciferase activity was measured. By comparing the ratio of IFN-inducible firefly luciferase/constitutively expressed renilla luciferase to mock-treated control, the neutralization capacity of Abs was determined. Supernatant of the in-house-produced anti-IFNα Ab, a commercial anti-IFNα Ab and anti-IFNω Ab were tested in the same assay. Abs were incubated for 1 hour with 1000 IU/mL IFNα2, 1000 IU/mL IFNω or DMEM, and the IFN-Ab mixture was added to the transfected cells (**Fig. 8b**). When only IFNα2 was added to transfected 293T cells, an increase in firefly luciferase expression was observed. Adding commercial anti-IFNα Ab with a dilution of 1:100 resulted in inhibition of the relative firefly luciferase expression. This neutralization capacity disappeared when more diluted Ab concentrations were used. The addition of an anti-IFNω Ab did not result in reduced expression of firefly luciferase when this Ab was pre-incubated with IFNα, therefore it was concluded that the anti-IFNω Ab was not cross-reactive against IFNα. For the in-house-produced anti-IFNα Ab, a dilution of 1:100 and 1:1000 resulted in complete inhibition of the luciferase expression. With a dilution of 1:10000, still some neutralizing capacity was observed. When the Abs were pre-incubated with IFNω and added to the cells, only a neutralizing effect of the anti-IFNω Ab was observed with a dilution of 1:100 (**Fig. 8c**). These results indicated that specific neutralizing Abs against IFNα (commercial and in-house-produced) or against IFNω were identified.

The same experimental set-up was used to test the neutralization capacity of anti-IFNß Abs. The anti-IFNß Ab PAb showed neutralization capacity with a dilution of 1:100 and 1:1000, whereas the other tested anti-IFNß Abs (MMHB-3 and MMHB-15) did not (**Fig. 8d**). The identified anti-IFNα Abs and anti-

IFNω Ab did not cross-react to IFNß. There was no cross-reactivity of the anti-IFNß Ab (PAb) to IFNω (**Fig. 8e**). Thus, neutralizing Abs against IFNα, IFNß, and IFNω were characterized, and these Abs could be used in follow-up experiments to assess the effect of blocking individual IFNs on virus replication.

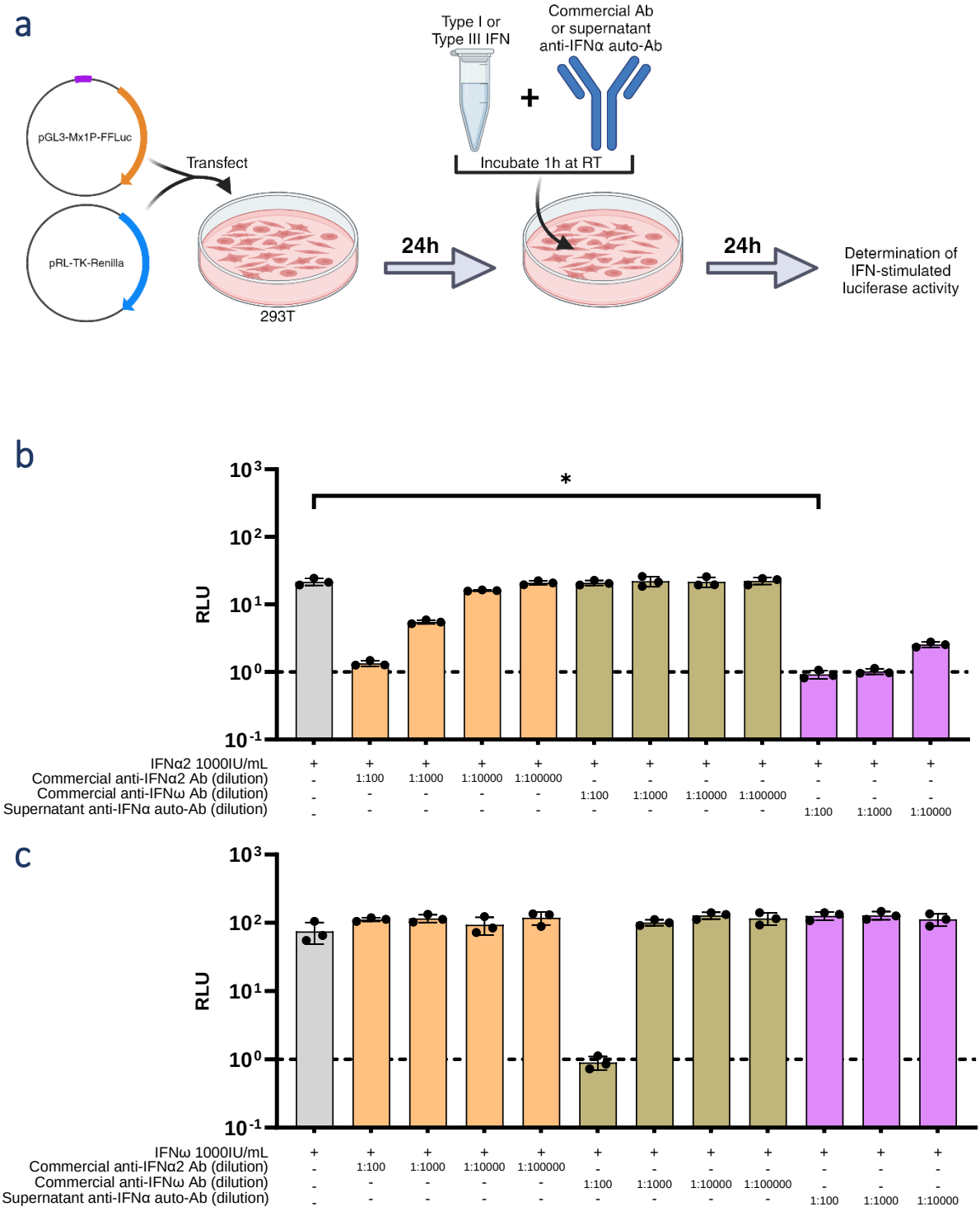

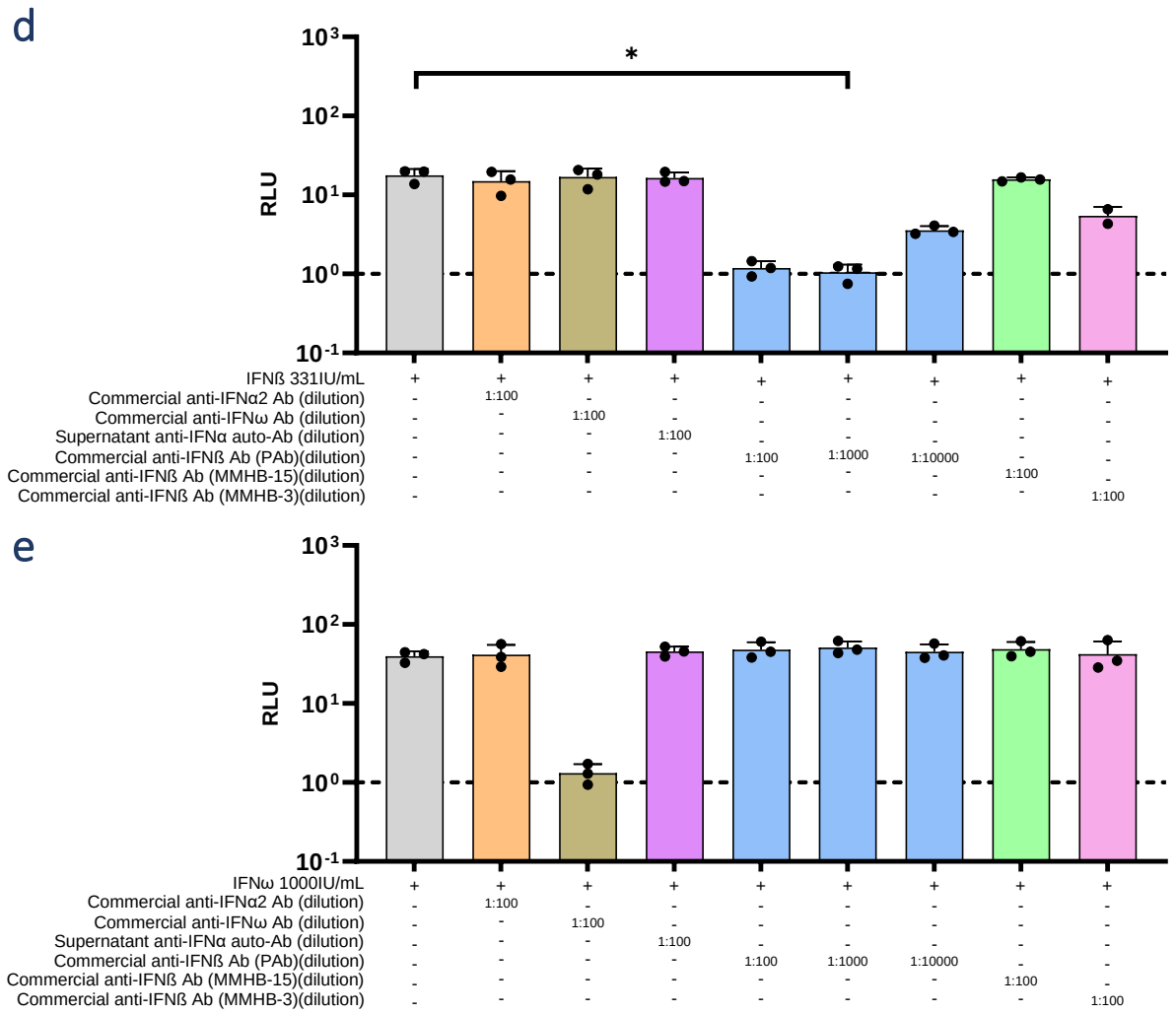

Fig. 8a-e. Characterization of neutralizing Abs against IFNα, IFNß, and IFNω. a) Schematic overview of the luciferase reporter-based IFN neutralization assay. 293T cells were transfected with luciferase-based IFN-reporter constructs, and a pre-incubated mixture of IFN and an anti-IFN Ab was added to the 293T cells. Twenty-four hours post-treatment, IFN-stimulated luciferase activity was quantified. Firefly luciferase values were normalized to Renilla luciferase values, and these values were compared to DMEM-stimulated 293T cells. Created with BioRender.com. **b-c)** Neutralization capacity of commercial anti-IFNα Ab, anti-IFNω Ab, and supernatant of in-house produced anti-IFNα Ab for 1000 IU/mL IFNα2 (**b**) or IFNω (**c**) was tested with the luciferase reporter-based neutralization assay. **d-e)** Neutralization capacity of commercial anti-IFNα Ab, anti-IFNω Ab, anti-IFNß Abs, and supernatant of in-house produced anti-IFNα Ab for 1000 IU/mL IFNß (**d**) or IFNω (**e**) was tested with the luciferase reporter-based neutralization assay.

CRISPR/Cas9-mediated knockout of IFNα, IFNß, IFNε, IFNκ, IFNω, IFNAR1, *and* IFNLR1

The second side-project aimed to generate knockouts of *IFNα* (all 13 *IFNα* genes), *IFNß*, *IFNε*, *IFNκ*, *IFNω*, *IFNAR1*, and *IFNLR1* in A549 2D8 cells using the CRISPR/Cas9 technology. CRISPR/Cas9-mediated knockout was determined by genomic sequencing of the targeted gene (NGS was performed by the diagnostics department of the Institute of Medical Virology, University of Zürich, Switzerland). CRISPR/Cas9-mediated knockout of *IFNß*, *IFNε*, *IFNκ*, *IFNω*, *IFNAR1*, and *IFNLR1* was straightforward, as only 1 gRNA per target was used. Knocking out all 13 *IFNα* genes in the same single cell clone was more complex. Three gRNAs targeting conserved regions of the *IFNα* genes were designed. These 3 gRNAs would in theory target all 13 *IFNα* genes, resulting in complete knockout of all *IFNα* genes. Initially, transfecting all three IFNα gRNAs at the same time was attempted, but the genome of the transfected A549 2D8 cells could not be sequenced. Therefore, another approach was used, which involved sequentially knocking out all 13 *IFNα* genes by transfecting 1 gRNA at a time. This approach would eventually lead to the complete knockout of all *IFNα* genes. Currently, several single cell clones

are available with a knockout of 4 *IFNα* genes. Knocking out the other *IFNα* genes in these single cell clones is still work in progress. For *IFNß* no single cell knockout clones were obtained with the used gRNA, and a new gRNA is needed for genomic knockout of *IFNß*. At least 2 clones with a 100% genomic knockout of *IFNε*, *IFNκ*, *IFNω*, *IFNAR1*, and *IFNLR1* were obtained (determined by NGS). An overview of the obtained single cell clones can be found in the supplementary materials (**Tab. S4**).

IFNAR1 and *IFNLR1* single cell knockout clones were also functionally tested. Three single clones that were confirmed by NGS to be *IFNAR1* knockouts (clones 1-1, 1-2, and 1-6), and one clone with a 21-nucleotide deletion (clone 1-5) were selected. For *IFNLR1*, at the time of performing the experiments, only 1 knockout single cell clone (clone 2-1) was available. One incomplete *IFNLR1* knockout (clone 2-2, 50% knockout), and two single cell clones with the wildtype *IFNLR1* sequence (clone 1-1, and 2-1) were included as controls. All single cell clones and the parental cell line (A549 2D8 cells) were stimulated with DMEM, 1000 IU/mL IFNα2, or 1000 IU/mL IFNλ1 for 16 hours. Cells were harvested, RNA was isolated, and ISG expression levels were quantified by RT-qPCR. The ISG expression levels were normalized to A549 2D8 cells stimulated with DMEM (**Fig. 9a-f**). When A549 2D8 cells were stimulated with IFNα2 or IFNλ1, an increase in mRNA expression was observed for all three tested ISGs. IFNα2 or IFNλ1 stimulation of *IFNAR1* single cell knockout clone 1-1 both resulted in an increase in ISG expression levels, even though this clone was a 100% genetic *IFNAR1* knockout clone as determined by NGS (**Fig. 9a-c**). For *IFNAR1* clone 1-5, which was a 50% genomic knockout, also an increase in ISGs expression levels was observed when stimulated with IFNα2 or IFNλ1 (**Fig. 9a-c**). The two *IFNAR1* single cell clones 1-2 and 1-6, which both were by NGS confirmed 100% *IFNAR1* knockouts, did only respond to IFNλ1 stimulation and not to IFNα2 stimulation (**Fig. 9a-c**). This suggested that *IFNAR1* single cell clones 1-2 and 1-6 did not contain a functional IFNAR1 protein, which was in line with the NGS data. The *IFNLR1* single cell clones 1-1, 1-2 and 2-2, all containing the wildtype genomic sequence for *IFNLR1,* did only respond to IFNα2 stimulation and not to IFNλ1 (**Fig. 9d-f**). This was unexpected as the parental cell line, A549 2D8 cells, did respond to IFNλ1 stimulation, indicating that these A549 2D8 and all wildtype derivatives should contain a functional IFNLR1 protein, which was not observed for the *IFNLR1* single cell clones 1-1, 1-2 and 2-2. The *IFNLR1* single cell clone 2-1, which was a by NGS confirmed *IFNLR1* knockout did only respond to IFNα2 stimulation and not to IFNλ1 stimulation, which was in line with the NGS data (**Fig. 9d-f**). After the unexpected results for the *IFNAR1* single cell clone 1-1 and the *IFNLR1* single cell clones 1-1, 1-2 and 2-1, all tested single cell clones were re-sequenced by NGS. *IFNAR1* clones 1-1, 1-2 and 1-6 were confirmed to be 100% genomic knockouts, whereas clone 1-5 again had the 21-nucleotides deletion. All *IFNLR1* single cell clones (1-1, 1-2, 2-1 and 2-2) were determined to be partial knockouts (knockout percentage ranging from 77-88%; results based on low number of sequencing reads). Based on the functional test and the NGS data of *IFNAR1* single cell clones, it was decided that further experiments would be performed using *IFNAR1* single cells clones 1-2 and 1-6 as these were both genomic and functional knockouts. In addition, all *IFNLR* single cell clones were regarded as functional *IFNLR* knockouts.

Due to the differences between the genomic data and functional data it was decided to analyze IFNAR1 and IFNLR1 protein levels by western blot. The parental A549 2D8 cell line, the 2 *IFNAR1* genomic and functional knockouts, and 3 *IFNLR1* functional knockout cells were included. Anti-IFNAR1 and anti-IFNLR1 Abs were used to detect the IFN receptor proteins. For the IFNAR1 blot, a lot of background bands were observed (**Fig. 9g**). The predicted size of IFNAR1 is 64 kDa, but due to glycosylation a protein size between 64 and around 100 kDa was expected. No obvious IFNAR1 band was visible in the lane of the A549 2D8 cells, and therefore no conclusions on protein levels could be made. IFNLR1 was detected in the parental cell line A549 2D8 cells at a height that matched the predicted size of the IFNLR1 (58 kDa) (**Fig. 9h**). This band however was not visible in the lanes containing the cell lysate of the *IFNAR1* single cell knockout clones 1-2 and 1-6. This was unexpected since these two single cells

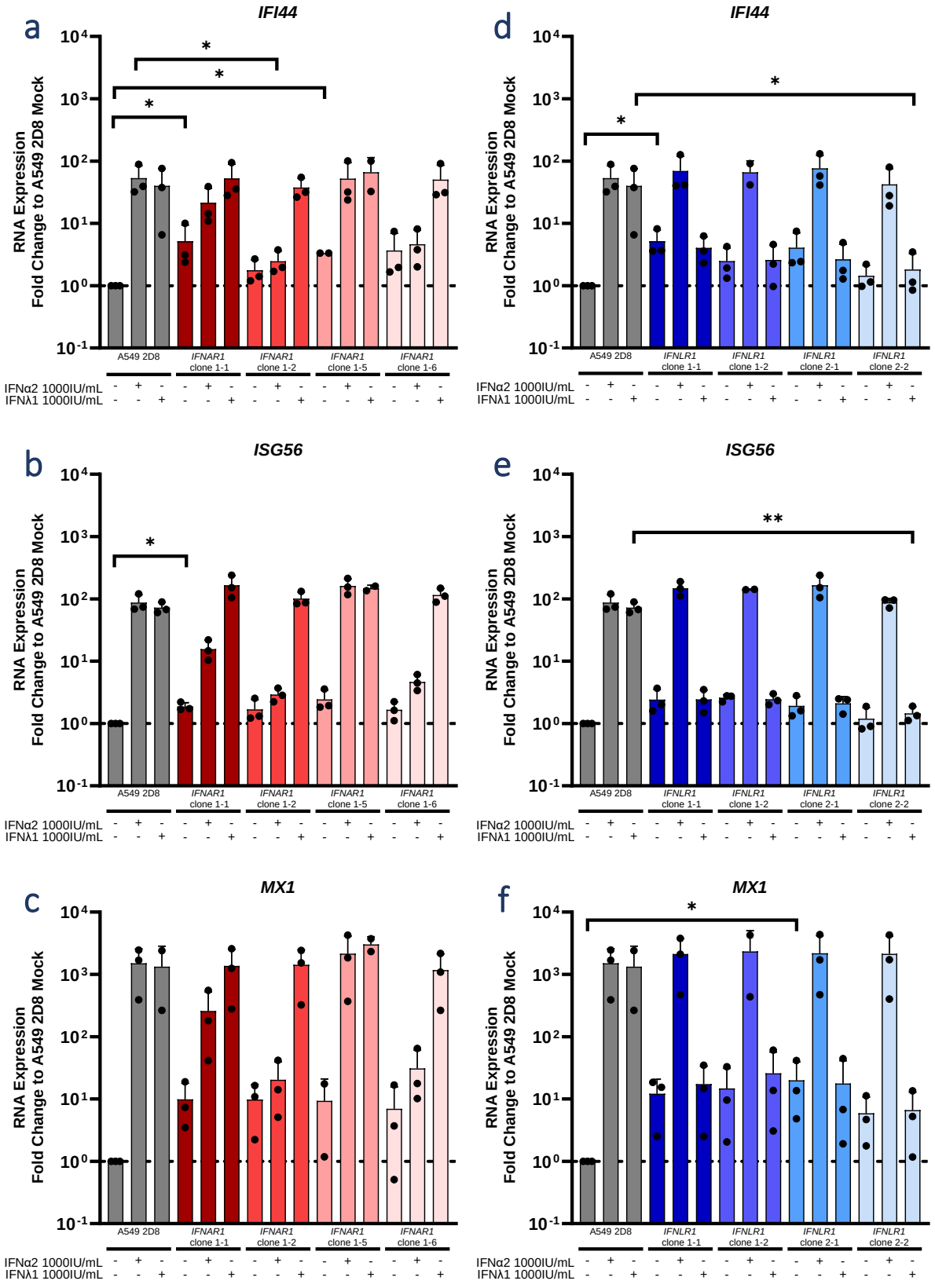
a
IFI44
RNA Expression
Fold Change to A549 2D8 Mock
A549 2D8
IFNAR1 clone 1-1
IFNAR1 clone 1-2
IFNAR1 clone 1-5
IFNAR1 clone 1-6
IFNα2 1000IU/mL
IFNλ1 1000IU/mL
d
IFI44
A549 2D8
IFNLR1 clone 1-1
IFNLR1 clone 1-2
IFNLR1 clone 2-1
IFNLR1 clone 2-2
b
ISG56
e
ISG56
c
MX1
f
MX1

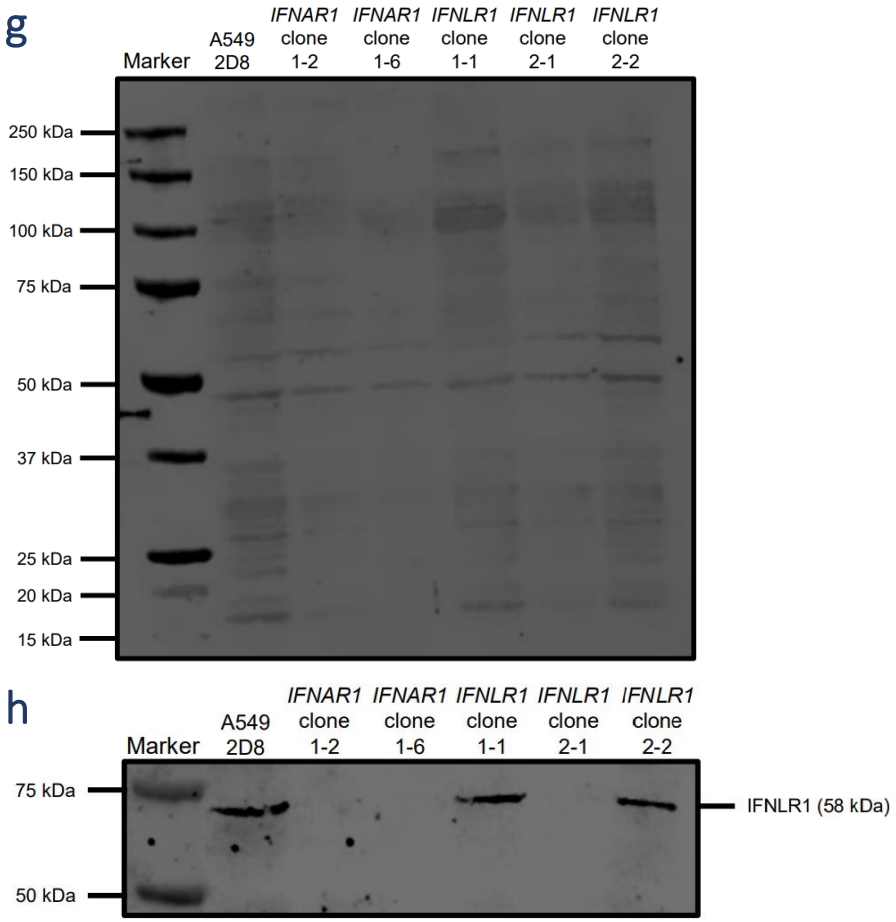

Fig. 9a-h. Characterization of *IFNAR1* and *IFNLR1* single cell knockout clones. a-f) A549 2D8 cells and selected *IFNAR1* and *IFNLR1* single cell clones were stimulated with 1000 IU/mL IFNα2, IFNλ1, or a similar volume of PBS in DMEM for 16 hours. Cells were harvested, RNA was isolated, and *IFI44* (**a**, **d**), *ISG56* (**b**, **e**), and *MX1* (**c**, **f**) mRNA expression levels were quantified by RT-qPCR. Values were normalized to unstimulated PBS-treated A549 2D8 cells. **g-h)** IFNAR1 and IFNLR1 protein levels in cell lysates of A549 2D8 cells and selected *IFNAR1* and *IFNLR1* single cell knockout clones were analyzed by western blot. IFNAR1 (**g**) and IFNLR1 (**h**) were detected with antibodies, and Precision Plus Protein™ All Blue Prestained Protein Standards was used as a marker.

clones did respond to IFNλ1 stimulation (**Fig. 9a-c**), indicating that these two single cell clones still expressed the IFNLR1. For the *IFNLR1* single cell clones, a band was visible for the 1-1 and the 2-2 clones. These two were only functional knockouts and not genomic knockouts. The detection of the IFNLR1 in these single cell clones was thus in line with the genomic data. For the *IFNLR1* single cell clone 2-1 no band was detected for IFNLR1, which was in line with the first sequencing results (100% genomic knockout), but not in line with the second sequencing results (not a complete genomic knockout). No loading control staining was performed (e.g. beta-actin). Overall, the western blot data did not clarify inconsistencies between the NGS data and the functional assay.

The *IFNAR1* and *IFNLR1* single cell clones were used for an infection experiment to assess the effect of type I and type III IFN signaling on virus replication. *IFNAR1* single cell clones 1-2 and 1-6, *IFNLR1* clones 1-1, 2-1 and 2-2, and the parental cell line A549 2D8 cells were inoculated with A/mallard/NY/78 with a MOI of 0.03 (**Fig. 10a**). No enhancement of virus replication was observed in any of the *IFNAR1* or *IFNLR1* single cell knockout clones. For some clones, a small reduction in replication was observed. Thus, with the used set-up, knockout of either *IFNAR1* or *IFNLR1* did not result in enhanced A/mallard/NY/78-replication in these single cell knockout clones.

Since no enhancement of A/mallard/NY/78-replication was observed in the *IFNAR1* and *IFNLR1* single cell knockout clones, a follow-up experiment was designed involving two GFP-expressing viruses. *IFNAR1* single cell knockout clones 1-2 and 1-6, *IFNLR1* single cell knockout clones 1-1, 1-2 and 2-2 were inoculated with PIV5-GFP and VSV-GFP. Similar to previous experiments, A549 2D8 cells treated with 5 µM ruxolitinib were included as a control. Cells were inoculated with a range of MOIs, and imaged over time by the Incucyte S3 live cell analysis instrument. For the analysis, the GFP-positive area (above a set threshold) was divided by the area covered by cells. The obtained percentage was a proxy for the percentage of infected cells over time. Consistent infection was only obtained when cells were inoculated with a MOI of 10 or 1, and therefore only these results were plotted (**Fig 10b-e**). For inoculation with PIV5-GFP with a MOI of 10, the percentage of infected cells over time differed between the cell lines from 35 h.p.i. onwards (**Fig. 10b**). The percentage of infected cells of both *IFNAR1* single cell knockout clones increased the fastest and to the highest percentage. However, the lack of enhancement of percentage of infected A549 2D8 cells upon treatment with ruxolitinib indicated that the observed differences for the *IFNAR1* and *IFNLR1* single cell clones were likely not caused by altered IFN signaling but were the result of clonal variability (**Fig. 10b**). Inoculation of the cell lines with PIV5-GFP with a MOI of 1, resulted in an enhanced percentage of infected cells of both *IFNAR1* single cell knockout clones over time (**Fig. 10c**). Again, this was likely the result of clonal variability, as the percentage of infected cells of ruxolitinib-treated A549 2D8 cells was comparable to the percentage of infected cells of DMSO-treated A549 2D8 cells over time.

The same experimental set-up was used for inoculation of A549 2D8 cells and selected *IFNAR1* and *IFNLR1* single cell knockout clones with VSV-GFP. Since the maximum percentage of infected cells was already observed at 34 h.p.i. (MOI 10) or at 43 h.p.i. (MOI 1) for all cell lines, the Green Area (%) was only plotted for the first 37 hours or 48 hours, respectively. (**Fig. 10d-e**). Treatment of A549 2D8 cells with ruxolitinib resulted in an enhanced percentage of VSV-GFP infected cells over time when cells were inoculated with a MOI of 10 (**Fig. 10d**). An even more rapid increase in percentage of infected cells was observed for all *IFNAR1* and *IFNLR1* single cells clones. Nevertheless, large error bars were observed due to the variability between most of the replicates, and therefore no conclusions could be drawn on the percentages of VSV-GFP-infected cells over time. The inoculation of cells with VSV-GFP with a MOI of 1 instead of a MOI of 10 resulted in comparable differences in the percentages of infected cells over time (**Fig. 10e**).

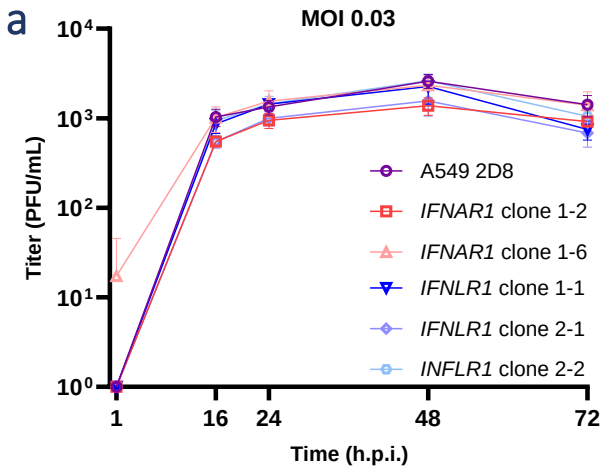

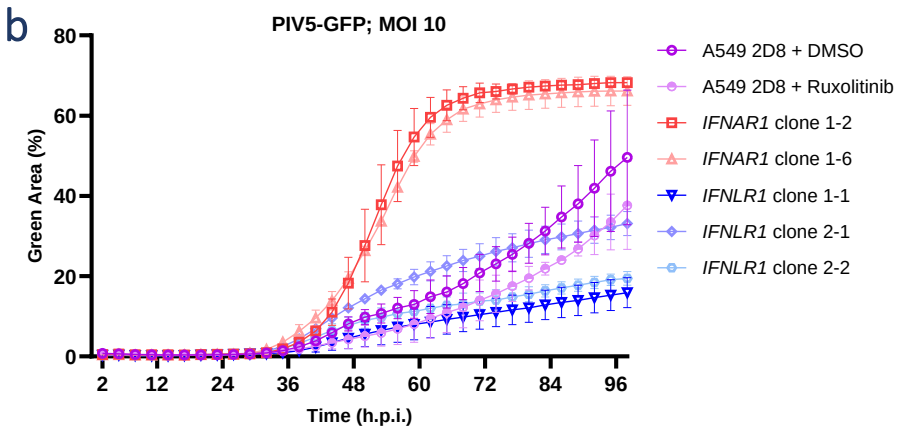
b
PIV5-GFP; MOI 10
Green Area (%)
Time (h.p.i.)
A549 2D8 + DMSO
A549 2D8 + Ruxolitinib
IFNAR1 clone 1-2
IFNAR1 clone 1-6
IFNLR1 clone 1-1
IFNLR1 clone 2-1
IFNLR1 clone 2-2

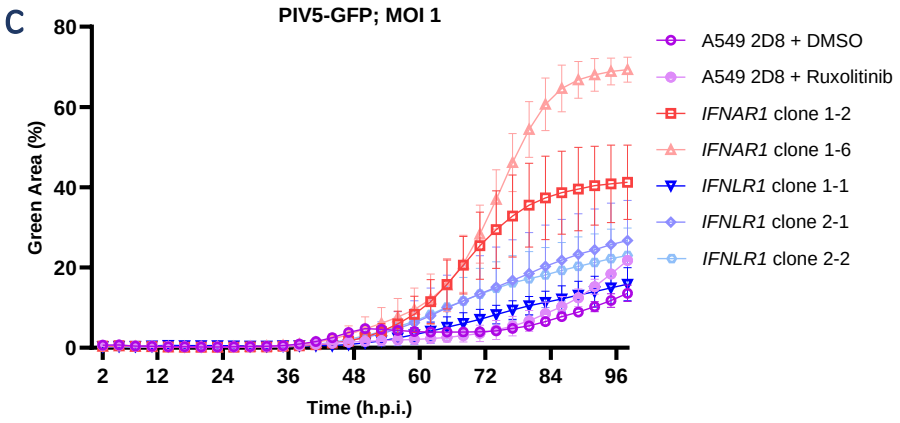
c
PIV5-GFP; MOI 1
Green Area (%)
Time (h.p.i.)
A549 2D8 + DMSO
A549 2D8 + Ruxolitinib
IFNAR1 clone 1-2
IFNAR1 clone 1-6
IFNLR1 clone 1-1
IFNLR1 clone 2-1
IFNLR1 clone 2-2

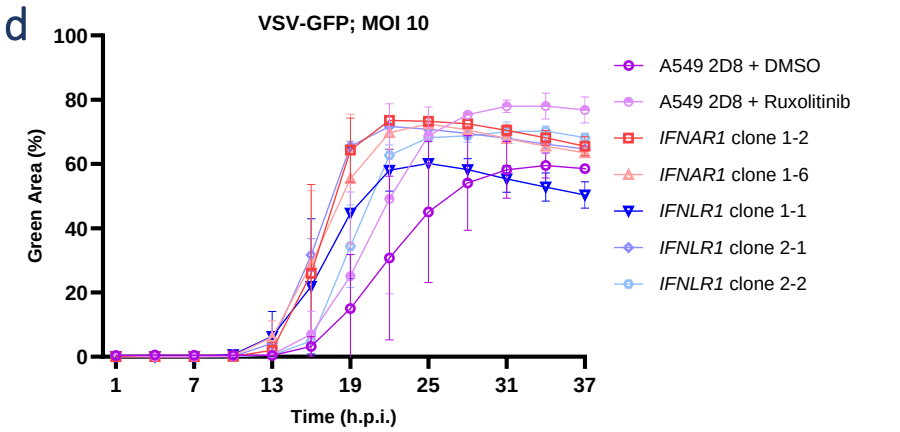
d
VSV-GFP; MOI 10
Green Area (%)
Time (h.p.i.)
A549 2D8 + DMSO
A549 2D8 + Ruxolitinib
IFNAR1 clone 1-2
IFNAR1 clone 1-6
IFNLR1 clone 1-1
IFNLR1 clone 2-1
IFNLR1 clone 2-2

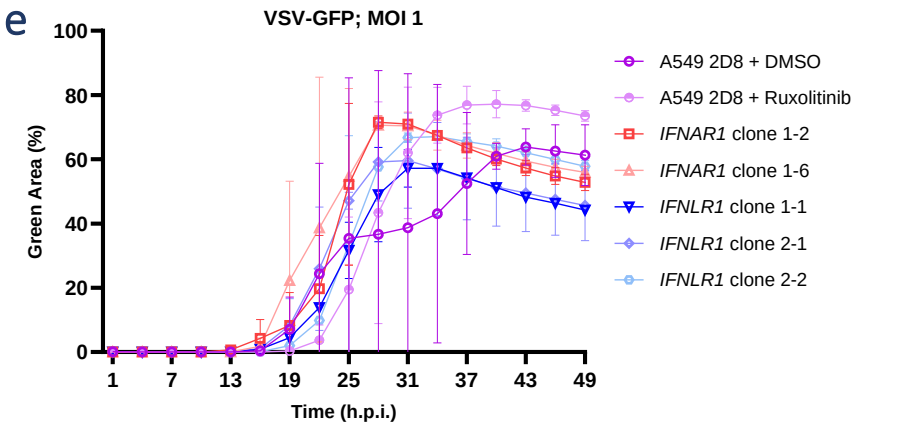
e
VSV-GFP; MOI 1
Green Area (%)
Time (h.p.i.)
A549 2D8 + DMSO
A549 2D8 + Ruxolitinib
IFNAR1 clone 1-2
IFNAR1 clone 1-6
IFNLR1 clone 1-1
IFNLR1 clone 2-1
IFNLR1 clone 2-2

Fig. 10a-e. Replication kinetics of A/mallard/NY/78, PIV5-GFP, and VSV-GFP in A549 2D8 cells and the *IFNAR1* and *IFNR1* single cell knockout clones. a) A549 2D8 cells and selected *IFNAR1* and *IFNLR1* single cell knockout clones were inoculated with A/mallard/NY/78 with a MOI of 0.03. Cells were treated with ruxolitinib or DMSO 1 h.p.i., and supernatant was harvested over time. Virus titers in the harvested supernatants were quantified by plaque assay. **b-e)** A549 2D8 cells and selected *IFNAR1* and *IFNLR1* single cell knockout clones were inoculated with PIV5-GFP with a MOI of 10 (**b**) or 1 (**c**), or inoculated with VSV-GFP with a MOI of 10 (**d**) or 1 (**e**). Cells were treated with ruxolitinib or DMSO 2 h.p.i. for PIV5-GFP inoculated cells and 1 h.p.i. for VSV-GFP inoculated cells. Cells were imaged over time using the Sartorius Incucyte S3 live cell analysis instrument. The GFP-positive area was divided by the area covered by cells to obtain Green Area (%).

Conclusion & Discussion

Many studies have been performed to investigate the relation between anti-IFN auto-Abs and viral disease ever since anti-IFN auto-Abs were detected in 10% of severe COVID-19 patients (*10*, *14–19*). However, studies on the molecular mechanisms of these anti-IFN auto-Abs are missing. In this report the set-up of an initial *in vitro* model system to study the effect of inhibition of the IFN system on IAV replication was described. The model system was developed to get a better understanding of the molecular mechanisms of anti-IFN auto-Abs and their relationship to virus replication. Furthermore, the model was used to determine which IFNs are produced upon virus infection, and thereby it was established which IFNs need to blocked to enhance IAV replication.

First, it was shown that 5 µm ruxolitinib was able to inhibit tonic and IFNα2-induced ISG expression levels in A549 and Calu-3 cells. This reduction has already been described for BEAS-2B cells, as treatment with 10 µM ruxolitinib for 24 hours resulted in reduced tonic and IFNß-induced ISG expression levels (*36*). Next, ruxolitinib-mediated enhancement of A/mallard/NY/78-replication was observed in both A549 cells and Calu-3 cells at all used MOIs, showing that A/mallard/NY/78-replication in these two cell lines is partially restricted by the IFN system. Ruxolitinib-mediated enhancement of virus replication has also been observed for SARS-CoV-2 in Vero E6 cells and Calu-3 cells, which indicates that ruxolitinib-mediated enhancement of replication is not virus specific (*34*, *35*). In follow-up experiments, ruxolitinib could be used to investigate how anti-IFN auto-Abs function and enhance virus replication. For example, it is not known whether blockage of virus-induced IFNs by anti-IFN auto-Abs is sufficient to obtain enhanced virus replication, or that tonic ISG expression levels should be reduced before an effect on virus replication is observed. A time of addition experiment with ruxolitinib should be performed to determine whether ruxolitinib-treatment can reduce tonic ISG expression levels and whether this affects virus replication.

Next, all three different methods used to quantify IFN mRNA expression levels or IFN protein levels in A549 cells upon infection with A/mallard/NY/78 showed that there was mainly mRNA expression and production of type III IFNs, and little to no mRNA expression and production of type I IFNs. For example, infection of A549 cells with A/mallard/NY/78 induced the mRNA expression of *IFNα2*, *IFNß IFNλ1* and *IFNλ2/3*. In contrast, only increased protein levels of IFNλ1 and IFNλ3 were detected, and not an increase in type I IFNs protein levels. This discrepancy could be the result of the sensitivity of the IFN detection kit that was used to quantify protein levels. To test this, samples containing known concentrations of IFN proteins should be included in follow-up experiments to validate the sensitivity of the IFN detection kit, and to accurately detect IFN proteins in the future. In addition, the discrepancy between the mRNA expression and protein levels could be caused by differences in the IFN response of the used A549 cells, as the experiments were not performed in parallel and different cell batches were used throughout these experiments. Changes in the IFN response could be caused by differences in cell passage number, number of cells seeded, number of infectious virus particles added, and time of storage of the cells and/or virus stock. To control for variability of cell batches, future experiments should preferably be performed in parallel, or at least shortly after one another using the same cell batch.

Another method used to quantify IFNs levels induced upon A/mallard/NY/78-infection was to compare ISG expression levels of infected A549 cells with ISGs expression levels of A549 cells stimulated with a concentration range of different IFNs. This comparison showed that ISG expression levels in A/mallard/NY/78-infected cells were comparable to ISG expression levels of A549 cells stimulated with 3-10 IU/mL IFNα2, 10-30 IU/mL IFNλ1, 1-10 IU/mL IFNß, or <1-10 IU/mL IFNω. These results indicated that higher concentrations of type III IFNs are required than type I IFNs to get similar ISG expression levels. These concentrations of IFNs were used in subsequent experiments to stimulate cells where the

IFN receptors were blocked by neutralizing antibodies. Incomplete inhibition of ISG expression levels by the anti-IFNAR and anti-IFNLR Abs was obtained when A549 cells were stimulated with 30 or 100 IU/mL IFNα2, or 30 IU/mL IFNλ1. Despite the incomplete inhibition, inoculation experiments were performed with Ab concentrations at which an adequate reduction in ISG expression levels was obtained. Enhanced A/mallard/NY/78-replication was observed when the IFNAR or IFNLR signaling alone was blocked. Contradictory, no effect on virus replication was observed when IFNAR and IFNLR were both blocked. Additionally, when the experiment was repeated twice, no consistent effect on A/mallard/NY/78-replication was observed when IFN signaling was blocked by one or both anti-IFN receptor Abs. This could indicate that the used concentrations of anti-IFNAR and anti-IFNLR Abs have not been optimized, and that higher Ab concentrations should be used. The experiments should therefore be repeated to identify anti-IFN receptor Ab concentrations at which complete inhibition of ISG expression levels are obtained. Additionally, ruxolitinib should be included as a control to ensure that complete inhibition can be obtained with the at that moment used IFN stock and cells.

Once the *in vitro* model system is optimized for the study of the effect of blockage of the IFNAR and/IFNLR signaling pathway, follow-up experiments to study the effect of blockage of individual IFNs on virus replication should be performed. In this report, commercially available neutralizing Abs against IFNα, IFNß, and IFNω were characterized. Neutralizing Abs against IFNλ1, IFNλ2, and IFNλ3 were characterized previously. In addition, a broadly neutralizing anti-IFNα auto-Ab cloned and produced in-house. The sequences of this anti-IFNα auto-Ab (19D11) were obtained from Meyer *et al*. (*30*). This antibody potently neutralized all 12 IFNα proteins tested, and it did not neutralize IFNß, IFNω and IFNγ (*30*). The cloning and production of this anti-IFNα auto-Ab serves as a proof-of-principle for the cloning of patient-derived anti-IFN auto-Abs, a method that could be used in the future to study the molecular properties of patient-derived anti-IFN auto-Abs.

As a model virus for this study, A/mallard/NY/78 was selected. However, other (influenza A) viruses might be more sensitive to IFN-mediated restriction of virus replication, and therefore could be more suitable for the *in vitro* model system to study anti-IFN auto-Abs. For example, anti-IFN auto-Abs are associated with severe COVID-19 and WNV encephalitis, and SARS-CoV-2 or WNV might therefore be a better model virus for the study of anti-IFN auto-Abs (*10*, *14–19*, *22*). In addition, A549 cells, the model cell line used in this report may be sub-optimal. There might be other cell lines cells that show larger IFN-mediated restriction of virus replication. This could include primary cells, that better mimic the human lung and may therefore serve as a better model. Optimizing the model cell line used for these studies could help to get a better understanding of the molecular mechanisms of anti-IFN auto-Abs and their relationship to virus replication.

The second project aimed to generate knockouts of *IFNα* (all 13 *IFNα* genes), *IFNß*, *IFNε*, *IFNκ*, *IFNω*, *IFNAR1*, and *IFNLR1* in A549 2D8 cells using the CRISPR/Cas-9 technology. A549 2D8 cells were used instead of normal A549 cells, because the intercellular variability for this cell line is smaller as this cell line was obtained by subcloning bulk A549 cells (*31*). However, variability between different single cell clones was still observed, as VSV-GFP and PIV5-GFP replicated differently in the 2 *IFNAR1* single cell knockout clones, and in the 3 *IFNLR1* single cell clones. Therefore, in follow-up experiments at least 3, but preferably more, single cell clones should be included to ensure that the observed effect is due to the knockout of the targeted gene and not the result of clonal variability. So far, at least 2 single cell knockout clones of *IFNε*, *IFNκ*, *IFNω*, *IFNAR1*, and *IFNLR1* were obtained. For the knockout of *IFNß*, no knockout clones were obtained yet and a new gRNA is needed. The knockout of *IFNα* is more complicated, as the genome of the cells transfected with all three *IFNα* gRNAs could not be sequenced. This could be due to the introduction of certain mutations that led to the loss of binding sites for the used primers, resulting in low to no PCR amplification and therefore a very low number of sequencing

reads. Additionally, it is possible that the introduction of multiple gRNAs led to more double strand breaks, resulting in the deletion of complete genomic parts. Therefore, another experimental strategy to knockout all 13 *IFNα* genes could be considered, for example the sequential knockout of the *IFNα* genes. However, this is an elaborate process, and sequential subcloning of each consecutive knockout will generate a cell line with very specific characteristics that potentially is distinct from the parental cell line. This might lead to lower or even loss of expression of the receptor or other host factors required for viral infection of cells. Another option would be to use Cas12 (Cpf1) instead of Cas9. Cas12 has been optimized for multiplexed genome engineering, and therefore all 13 *IFNα* genes could potentially be knocked out after only one transfection (*37*). This would help to overcome the sequential selection of single cell clones.

A limitation of the second project is the inconsistency between the genomic, functional and western blot data of the *IFNAR1* and *IFNLR1* single cell clones. Knockout of the targeted genes was initially tested by NGS, and if possible, followed up by a functional test. The results from these two approaches did not always match. For example, *IFNAR1* and *IFNRL1* single cell clones that were determined to be a knockout by sequencing were not a functional knockout, or vice versa. This inconsistency could potentially be explained by biases in the NGS pipeline towards certain sequences. In support of this, for some single cell knockout samples a low number of NGS reads was obtained, and these samples should therefore be re-sequenced in order to validate the genomic knockout data. In addition, dysfunctional single cell clones with a genome matching the reference sequence may have had a different phenotype than the parental cell line, which potentially resulted in reduced or no expression of *IFNAR1* or *IFNLR1*, causing unresponsiveness to IFN stimulation. Besides, it could be that the introduced frameshift did not lead to the knockout of *IFNAR1* or *IFNLR1*, causing the single cell clones to express an altered but functional receptor.

In an attempt to validate the *IFNAR1* and *IFNLR1* single cell knockout clones, IFNAR1 and IFNLR1 protein levels of single cell clones were analyzed. IFNAR1 could not be detected on the western blot and therefore no conclusions could be drawn on IFNAR1 protein levels. In addition, the IFNLR1 protein levels of the single cell clones did not clarify the differences between the genomic and functional data. Therefore, optimization of the western blot protocol is required, before the data can be used to help determine which single cell clones are actual knockouts. Moreover, the addition of a loading control (*e.g*. ß-actin) would also improve the western blot data. The observation that the genomic data of the *IFNAR1* and *IFNLR1* single cell clones did not always match the functional data and/or western blot data indicates that the genomic, functional and western blot data of the single cell clones should be handled with caution, and that single cell clones should always be functionally tested after they are sequenced by NGS. If a single cell clone is both a genomic knockout and a functional knockout, it can be regarded with certainty as an actual single cell knockout clone. In this study, 2 *IFNAR1* single cell knockout clones (1-2 and 1-6) and 1 *IFNLR1* single cell knockout clone (2-1) that were both a genomic and functional knockout were identified, and these single cell knockout clones were used for follow-up experiments. In addition, 2 *IFNLR1* single cell clones (1-1 and 2-2) that were only a functional knockout were also included.

Compared to A549 2D8 cells, no enhancement of A/mallard/NY/78-replication was observed in the *IFNAR1* and *IFNLR1* single cell knockout clones. This suggested that inhibition of IFNAR or IFNLR signaling had no effect on the replication of A/mallard/NY/78, which was also observed when commercial Abs were used to block the IFNAR and/or IFNLR. The lack of enhancement of A/mallard/NY/78-replication in the *IFNAR1* and *IFNLR1* single cell knockout clones adds to the idea that avian IAV A/mallard/NY/78 may not be the optimal model virus for the study of anti-IFN auto-Abs.

Since no enhancement of A/mallard/NY/78-replication in the *IFNAR1* and *IFNLR1* single cell knockout clones was observed, a different experimental approach using PIV5-GFP and VSV-GFP was used to determine whether the knockout of *IFNAR1* or *IFNLR1* in A549 2D8 cells could enhance virus replication. In a preliminary experiment, large variability in replication between the different cells was observed for both viruses, regardless of whether these cells had a functional IFNAR or IFNLR. In addition, treatment of A549 2D8 with ruxolitinib did not result in enhanced replication of these viruses. Consequently, the observed differences are likely the result of clonal variability rather than altered IFN signaling.

Overall, this report described the set-up and use of an initial *in vitro* model system to study the effect of inhibition of the IFN system on IAV replication. Experiments were performed to identify IFN-sensitive viruses, characterize neutralizing Abs and an IFN signaling inhibitor, quantify IFN production upon virus infection, and generate knockout cells. These assays and tools can be used to improve the initial *in vitro* model system used in this report. Follow-up experiments should focus on the identification of highly IFN-sensitive viruses and characterization of cell lines or primary cells that show large IFN-mediated restriction of virus replication. Once established, the improved *in vitro* model system can be used to study the molecular mechanisms of anti-IFN auto-Abs and their relationship to virus replication.

References

1. E. V. Mesev, R. A. LeDesma, A. Ploss, Decoding type I and III interferon signalling during viral infection. *Nat Microbiol* **4**, 914–924 (2019).

2. L. Dalskov, H. H. Gad, R. Hartmann, Viral recognition and the antiviral interferon response. *EMBO J* **42**, e112907 (2023).

3. A. Isaacs, J. Lindenmann, Virus interference. I. The interferon. *Proc R Soc Lond B Biol Sci* **147**, 258–267 (1957).

4. J. Lindenmann, D. C. Burke, A. Isaacs, Studies on the Production, Mode of Action and Properties of Interferon. *Br J Exp Pathol* **38**, 551–562 (1957).

5. J. W. Schoggins, Interferon-Stimulated Genes: What Do They All Do? *Annu Rev Virol* **6**, 567–584 (2019).

6. H. M. Lazear, J. W. Schoggins, M. S. Diamond, Shared and Distinct Functions of Type I and Type III Interferons. *Immunity* **50**, 907–923 (2019).

7. A. M. Gocher, C. J. Workman, D. A. A. Vignali, Interferon-γ: teammate or opponent in the tumour microenvironment? *Nat Rev Immunol* **22**, 158–172 (2021).

8. E. Alspach, D. M. Lussier, R. D. Schreiber, Interferon γ and Its Important Roles in Promoting and Inhibiting Spontaneous and Therapeutic Cancer Immunity. *Cold Spring Harb Perspect Biol* **11**, a028480 (2019).

9. H. C. Su, H. Jing, Y. Zhang, J. L. Casanova, Interfering with Interferons: A Critical Mechanism for Critical COVID-19 Pneumonia. *Annu Rev Immunol* **41**, 561–585 (2023).

10. P. Bastard, L. B. Rosen, Q. Zhang, E. Michailidis, *et al*., Autoantibodies against type I IFNs in patients with life-threatening COVID-19. *Science* **370**, eabd4585 (2020).

11. S. Dupuis, E. Jouanguy, S. Al-Hajjar, C. Fieschi, *et al*., Impaired response to interferon-alpha/beta and lethal viral disease in human STAT1 deficiency. *Nat Genet* **33**, 388–391 (2003).

12. N. Hernandez, G. Bucciol, L. Moens, J. Le Pen, *et al*., Inherited IFNAR1 deficiency in otherwise healthy patients with adverse reaction to measles and yellow fever live vaccines. *J Exp Med* **216**, 2057–2070 (2019).

13. J. L. Casanova, M. S. Anderson, Unlocking life-threatening COVID-19 through two types of inborn errors of type I IFNs. *J Clin Invest* **133**, e166283 (2023).

14. P. Bastard, A. Gervais, T. Le Voyer, J. Rosain, *et al*., Autoantibodies neutralizing type I IFNs are present in ~4% of uninfected individuals over 70 years old and account for ~20% of COVID-19 deaths. *Sci Immunol* **6**, 4340–4359 (2021).

15. I. Busnadiego, I. A. Abela, P. M. Frey, D. A. Hofmaenner, *et al*., Critically ill COVID-19 patients with neutralizing autoantibodies against type I interferons have increased risk of herpesvirus disease. *PLoS Biol* **20**, e3001709 (2022).

16. X. Wang, Q. Tang, H. Li, H. Jiang, *et al*., Autoantibodies against type I interferons in COVID-19 infection: A systematic review and meta-analysis. *Int J Infect Dis* **130**, 147–152 (2023).

17. M. G. P. van der Wijst, S. E. Vazquez, G. C. Hartoularos, P. Bastard, *et al*., Type I interferon autoantibodies are associated with systemic immune alterations in patients with COVID-19. *Sci Transl Med* **13**, eabh2624 (2021).

18. F. Frasca, M. Scordio, L. Santinelli, L. Gabriele, *et al*., Anti-IFN-α/-ω neutralizing antibodies from COVID-19 patients correlate with downregulation of IFN response and laboratory biomarkers of disease severity. *Eur J Immunol* **52**, 1120–1128 (2022).

19. B. Akbil, T. Meyer, P. Stubbemann, C. Thibeault, *et al*., Early and Rapid Identification of COVID-19 Patients with Neutralizing Type I Interferon Auto-antibodies. *J Clin Immunol* **42**, 1111–1129 (2022).

20. Q. Zhang, A. Pizzorno, L. Miorin, P. Bastard, *et al*., Autoantibodies against type I IFNs in patients with critical influenza pneumonia. *J Exp Med* **219**, e20220514 (2022).

21. P. Bastard, E. Michailidis, H. H. Hoffmann, M. Chbihi, *et al*., Auto-antibodies to type I IFNs can underlie adverse reactions to yellow fever live attenuated vaccine. *J Exp Med* **218**, e20202486 (2021).

22. A. Gervais, F. Rovida, M. A. Avanzini, S. Croce, *et al*., Autoantibodies neutralizing type I IFNs underlie West Nile virus encephalitis in ∼40% of patients. *J Exp Med* **220**, e20230661 (2023).

23. B. Pozzetto, K. E. Mogensen, M. G. Tovey, I. Gresser, Characteristics of Autoantibodies to Human Interferon in a Patient with Varicella-Zoster Disease. *J Infect Dis* **150**, 707–713 (1984).

24. B. G. Hale, Autoantibodies targeting type I interferons: Prevalence, mechanisms of induction, and association with viral disease susceptibility. *Eur J Immunol* **53**, e2250164 (2023).

25. M. Vanker, K. Särekannu, A. Fekkar, S. E. Jørgensen, *et al*., Autoantibodies Neutralizing Type III Interferons Are Uncommon in Patients with Severe Coronavirus Disease 2019 Pneumonia. *J Interferon Cytokine Res* **43**, 379–393 (2023).

26. S. C. Lin, F. R. Zhao, H. Janova, A. Gervais, *et al*., Blockade of interferon signaling decreases gut barrier integrity and promotes severe West Nile virus disease. *Nat Commun* **14**, 5973 (2023).

27. F. Alotaibi, N. K. Alharbi, L. B. Rosen, A. Y. Asiri, *et al*., Type I interferon autoantibodies in hospitalized patients with Middle East respiratory syndrome and association with outcomes and treatment effect of interferon beta-1b in MIRACLE clinical trial. *Influenza Other Respir Viruses* **17**, e13116 (2023).

28. C. Meisel, B. Akbil, T. Meyer, E. Lankes, *et al*., Mild COVID-19 despite autoantibodies against type I IFNs in autoimmune polyendocrine syndrome type 1. *J Clin Invest* **131**, e150867 (2021).

29. J. Lopez, M. Mommert, W. Mouton, A. Pizzorno, *et al*., Early nasal type I IFN immunity against SARS-CoV-2 is compromised in patients with autoantibodies against type I IFNs. *J Exp Med* **218**, e20211211 (2021).

30. S. Meyer, M. Woodward, C. Hertel, P. Vlaicu, *et al*., AIRE-Deficient Patients Harbor Unique High-Affinity Disease-Ameliorating Autoantibodies. *Cell* **166**, 582–595 (2016).

31. J. Börold, D. Eletto, I. Busnadiego, N. K. Mair, *et al*., BRD9 is a druggable component of interferon-stimulated gene expression and antiviral activity. *EMBO Rep* **22**, e52823 (2021).

32. K. J. Livak, T. D. Schmittgen, Analysis of relative gene expression data using real-time quantitative PCR and the 2(-Delta Delta C(T)) Method. *Methods* **25**, 402–408 (2001).

33. A. Quintás-Cardama, K. Vaddi, P. Liu, T. Manshouri, *et al*., Preclinical characterization of the selective JAK1/2 inhibitor INCB018424: therapeutic implications for the treatment of myeloproliferative neoplasms. *Blood* **115**, 3109–3117 (2010).

34. U. Felgenhauer, A. Schoen, H. H. Gad, R. Hartmann, *et al*., Inhibition of SARS–CoV-2 by type I and type III interferons. *J Biol Chem* **295**, 13958–13964 (2020).

35. S. Schroeder, F. Pott, D. Niemeyer, T. Veith, *et al*., Interferon antagonism by SARS-CoV-2: a functional study using reverse genetics. *Lancet Microbe* **2**, e210–e228 (2021).

36. D. Panda, E. Gjinaj, M. Bachu, E. Squire, *et al*., IRF1 maintains optimal constitutive expression of antiviral genes and regulates the early antiviral response. *Front Immunol* **10**, 1019 (2019).

37. C. C. Campa, N. R. Weisbach, A. J. Santinha, D. Incarnato, *et al*., Multiplexed genome engineering by Cas12a and CRISPR arrays encoded on single transcripts. *Nat Methods* **16**, 887–893 (2019).

Supplementary Materials

Tab. S1. List of RT-qPCR primers used in this study.

Gene	Use	FW/RV	Sequence (5' → 3')
18s rRNA	RT-qPCR	FW	GGCCCTGTAATTGGAATGACTC
		RV	CCAAGATCCAACTACGAGCTT
Actin	RT-qPCR	FW	GTTGCTATCCAGGCTGTGC
		RV	AATGTCACGCACGATTTCCCG
IFI44	RT-qPCR	FW	TGCTCTTTCTGACATCTCGGT
		RV	CCTCCCTTAGATTCCCTATTT
ISG56	RT-qPCR	FW	CTGTGGTAGGCTCTGCTTCC
		RV	CCACCACACCCAGCTAAGTT
MX1	RT-qPCR	FW	AGACAAGGTTGTGGACGTGG
		RV	TTCCTCCAGCAGATCCCTGA
RSAD2	RT-qPCR	FW	CCCCAACCAGCGTCAACTAT
		RV	TGATCTTCTCCATACCAGCTTCC
IFNα2	RT-qPCR	FW	CTTGAAGGACAGACATGACTTTGGA
		RV	GGATGGTTTCAGCCTTTTGGA
IFNß	RT-qPCR	FW	CATTACCTGAAGGCCAAGGA
		RV	CAGCATCTGCTGGTTGAAGA
IFNε	RT-qPCR	FW	AGCACTCATGGGACTGGAACTGGAAG
		RV	CAGGTGCTGTAGTCCTGGTT
IFNκ	RT-qPCR	FW	GCCCCAAGAGTTTCTGCAATAC
		RV	GGCCTGTAGGGACATTTCATAGA
IFNω	RT-qPCR	FW	GGAACACCTTGGTGCTTCTG
		RV	GTGGAGTTGGTCTAGGAGGG
IFNλ1	RT-qPCR	FW	GGTGACTTTGGTGCTAGGCT
		RV	TGAGTGACTCTTCCAAGGCG
IFNλ2	RT-qPCR	FW	AATTGTGTTGCCAGTGGGGA
		RV	GCGACTGGGTGGCAATAAAT

Tab. S2. Sequences of heavy and light chain of the in-house cloned and produced anti-IFNα auto-Ab.

Name	Use	Sequence (5' → 3')
Anti-IFNα auto-Ab Heavy Chain	In-Fusion Ab Cloning	GAGGTGCAGCTGTTGGAGTCTGGGGCTGAGGTGAAGAGGCCTGGGTCGTCGGTGAGGG TCTCCTGCAGGGCTTCTGGAGACACCTTCAGCAGTTACCCTATCAGTTGGGTGCGACAGGC CCCTGGACAAGGCCTTGAGTGGATGGGAAGGATCCTCCCTGCCCTTGGTGTCACAAACTA CGCTCAGAACTTCCGGGGCAGAATCACGATTACCGCGGACAAGTCGCCCCTCACAGCCTA CTTGGAACTGAGTAGCCTCAGATTTGAGGACACGGCCGTGTATTACTGTGCGAGTCCCAGT GCGGACAT AATTCCTTCGATTTTGGGGACGACCCTCTTTGCCTTCTGGGGCCAGGGAAGC CTGGTCACCGTCTCCTCA
Anti-IFNα auto-Ab Light Chain	In-Fusion Ab Cloning	GAAATTGTGTTGACGCAGTCTCCAGGCACCCTGTCTCTGTCTCCGGGGGAAGGGGCCACC CTCTCCTGCAGGGCCAGTCAGAATGTTAGCAGACACTACTTAACCTGGTACCAGCAGAAAC CTGGCCAGTCTCCCCGGCTCCTCATCTATGGTGGCTCCAGCAGGGCCACTGGCGTCCCAGA CAGGTTCAGTGGCGGTGGGTCTGGGACAGACTTCACTCTCACCATCAGCAGGCTGGAGCC TGAAGACTTTGCAGTGTTTTACTGCCAGAGCTATCATAGCCCACCTCCTGTGTACACTTTCG GCCAGGGGACCAAGGTGGAGATCAAA

Tab. S3. List of CRISPR/Cas9 crRNAs, NGS primers, and NGS barcodes used in this study.

Name/Gene	Use	FW/RV	Sequence (5' → 3')
IFNα gRNA1	CRISPR-Cas9 crRNA		TGATGGCAACCAGTTCCAGA
IFNα gRNA2	CRISPR-Cas9 crRNA		CTTCAATCTCTTCAGCACAA
IFNα gRNA3	CRISPR-Cas9 crRNA		CATCTCATGGAGGACAGAGA

IFNß	CRISPR-Cas9 crRNA		GTGGCAATTGAATGGGAGGC
IFNε	CRISPR-Cas9 crRNA		TAGACACTGCTGAATTGACA
IFNκ	CRISPR-Cas9 crRNA		CGTTCAGTAAGTTACAGTCC
IFNω	CRISPR-Cas9 crRNA		GGCTATAGCTGGTCATCACT
IFNLR1	CRISPR-Cas9 crRNA		GCGGCTGCGGACAACACCCA
IFNAR1	CRISPR-Cas9 crRNA		ACAAGTTCAAGGGACGCGTG
IFNα1 & IFNα13	NGS	FW	CTTTCCCTACACGACGCTCTTCCGATCTACAAATGAGCAGAATCTCTC
		RV	GACTGGAGTTCAGACGTGTGCTCTTCCGATCTTCATCCCAAGCAGCAGATGA
IFNα2	NGS	FW	CTTTCCCTACACGACGCTCTTCCGATCTGGAGTTTGGCAACCAGTTCC
		RV	GACTGGAGTTCAGACGTGTGCTCTTCCGATCTGCTGGTAGAGTTCAGTGTAG
IFNα4	NGS	FW	CTTTCCCTACACGACGCTCTTCCGATCTCTGCCTGAAGGACAGACATG
		RV	GACTGGAGTTCAGACGTGTGCTCTTCCGATCTTCTAGGAGGCTCTGTTCCCA
IFNα5	NGS	FW	CTTTCCCTACACGACGCTCTTCCGATCTACAAATGGGAAGAATCTCTC
		RV	GACTGGAGTTCAGACGTGTGCTCTTCCGATCTTCATCCCAAGTAGCAGATGA
IFNα6	NGS	FW	CTTTCCCTACACGACGCTCTTCCGATCTACAAATGAGGAGAATCTCTC
		RV	GACTGGAGTTCAGACGTGTGCTCTTCCGATCTTCATCCCAAGCAACAGATGA
IFNα7	NGS	FW	CTTTCCCTACACGACGCTCTTCCGATCTCTGCTTGAAGGACAGACATG
		RV	GACTGGAGTTCAGACGTGTGCTCTTCCGATCTTCTAGGAGGCTCTGTTCCCA
IFNα8	NGS	FW	CTTTCCCTACACGACGCTCTTCCGATCTCTGCCTGAAGGACAGACATG
		RV	GACTGGAGTTCAGACGTGTGCTCTTCCGATCTTCTAGAAGGGTCTCATCCAA
IFNα10	NGS	FW	CTTTCCCTACACGACGCTCTTCCGATCTACAAATGGGAAGAATCTCTC
		RV	GACTGGAGTTCAGACGTGTGCTCTTCCGATCTTGTTCCCAAGCAGCAGATGA
IFNα14	NGS	FW	CTTTCCCTACACGACGCTCTTCCGATCTCTGCCTGAAGGACAGACATG
		RV	GACTGGAGTTCAGACGTGTGCTCTTCCGATCTTCTAGGAGGGTCTCATCCCA
IFNα16	NGS	FW	CTTTCCCTACACGACGCTCTTCCGATCTACAAATGGGAAGAATCTCTC
		RV	GACTGGAGTTCAGACGTGTGCTCTTCCGATCTTCATCCCAAGCAGCAGATGA
IFNα17	NGS	FW	CTTTCCCTACACGACGCTCTTCCGATCTCTGCCTGAAGGACAGACATG
		RV	GACTGGAGTTCAGACGTGTGCTCTTCCGATCTTCTAGGAGGCTCTGTTCCCA
IFNα21	NGS	FW	CTTTCCCTACACGACGCTCTTCCGATCTACAAATGGGAAGAATCTCTC
		RV	GACTGGAGTTCAGACGTGTGCTCTTCCGATCTTGTTCCCAAGTAGCAGATGA
IFNß	NGS	FW	CTTTCCCTACACGACGCTCTTCCGATCTCTCTTTCCATGAGCTACAAC
		RV	GACTGGAGTTCAGACGTGTGCTCTTCCGATCTATGCGGCGTCCTCCTTCTGG
IFNε	NGS	FW	CTTTCCCTACACGACGCTCTTCCGATCTGAAACTGATTATCTTCCAGC
		RV	GACTGGAGTTCAGACGTGTGCTCTTCCGATCTGAGTGTGTCCTTTTTGGTAC
IFNκ	NGS	FW	CTTTCCCTACACGACGCTCTTCCGATCTTGATTCAAAAGTGTTTGTGG
		RV	GACTGGAGTTCAGACGTGTGCTCTTCCGATCTTTCTACAGGAAATGAATTGC
IFNω	NGS	FW	CTTTCCCTACACGACGCTCTTCCGATCTCAGTAAAGCCAGGAGCATCC
		RV	GACTGGAGTTCAGACGTGTGCTCTTCCGATCTGAAGCACCAAGGTGTTCCTG
IFNAR1	NGS	FW	CTTTCCCTACACGACGCTCTTCCGATCTCCCAGATGATGGTCGTCCTC
		RV	GACTGGAGTTCAGACGTGTGCTCTTCCGATCTTAGCCCAGCTGCGTGCCCTA
IFNLR1	NGS	FW	CTTTCCCTACACGACGCTCTTCCGATCTAGAGTGTGCGGGAACCAAGG
		RV	GACTGGAGTTCAGACGTGTGCTCTTCCGATCTTCAGTCCCTTACCCACAGAC
D501	NGS barcode		TATAGCCT
D502	NGS barcode		ATAGAGGC
D503	NGS barcode		CCTATCCT
D504	NGS barcode		GGCTCTGA
D505	NGS barcode		AGGCGAAG
D506	NGS barcode		TAATCTTA
D507	NGS barcode		CAGGACGT
D508	NGS barcode		GTACTGAC
D701	NGS barcode		ATTACTCG
D702	NGS barcode		TCCGGAGA
D703	NGS barcode		CGCTCATT
D704	NGS barcode		GAGATTCC

D705	NGS barcode		ATTCAGAA
D706	NGS barcode		GAATTCGT
D707	NGS barcode		CTGAAGCT
D708	NGS barcode		TAATGCGC
D709	NGS barcode		CGGCTATG
D710	NGS barcode		TCCGCGAA
D711	NGS barcode		TCTCGCGC
D712	NGS barcode		AGCGATAG

Tab. S4. Overview of generated single cell knockout clones.

Gene	NGS-confirmed single cell 100% knockout clones (#; knocked-out *IFNα* genes)
IFNα	g1:1-4 (α1, α5, α13), g1:1-14 (α5, α14), g1&3:1-7 (α1, α5, α13, α14), g1&3:1-9 (α1, α5, α13, α14)
IFNß	None
IFNε	1-2, 2-2, 2-3
IFNκ	2-1, 2-2, 2-3
IFNω	1-1, 2-1 (low number of reads)
IFNAR1	1-1, 1-2, 1-6
IFNLR1	2-1, 3-1, 3-2, 3-3, 3-4, 3-5, 3-7, 3-10, 3-12, 3-13, 3-14, 3-15, 3-16, 3-18

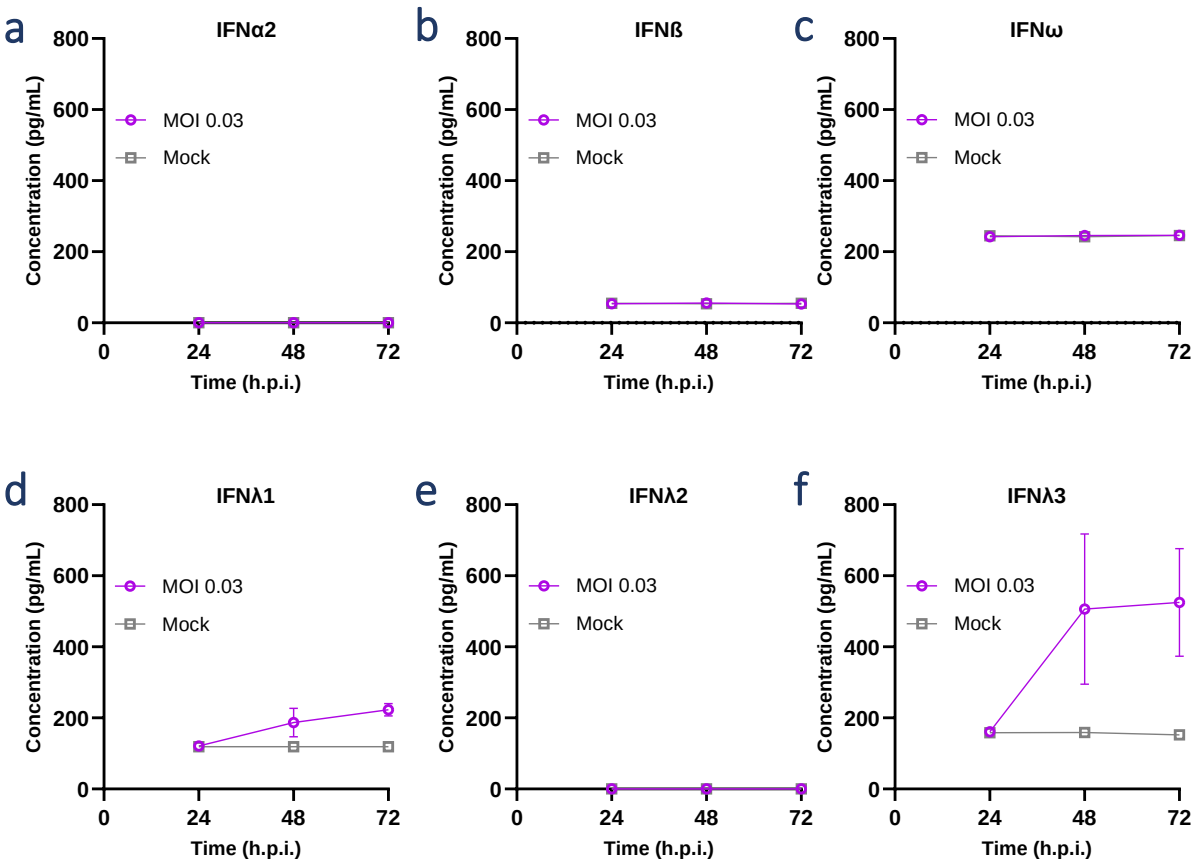

Fig. S1a-f. Production of type I and type III IFNs upon A/mallard/NY/78-infection in A549 cells. a-f) A549 cells were inoculated with A/mallard/NY/78 with a MOI of 0.03. Mock-infected A549 cells were included as a control. Supernatant was harvested over time and used to quantify IFNα2 (**a**), IFNß (**b**), IFNω (**c**), IFNλ1 (**d**), IFNλ2 (**e**), and IFNλ3 (**f**) protein concentrations.

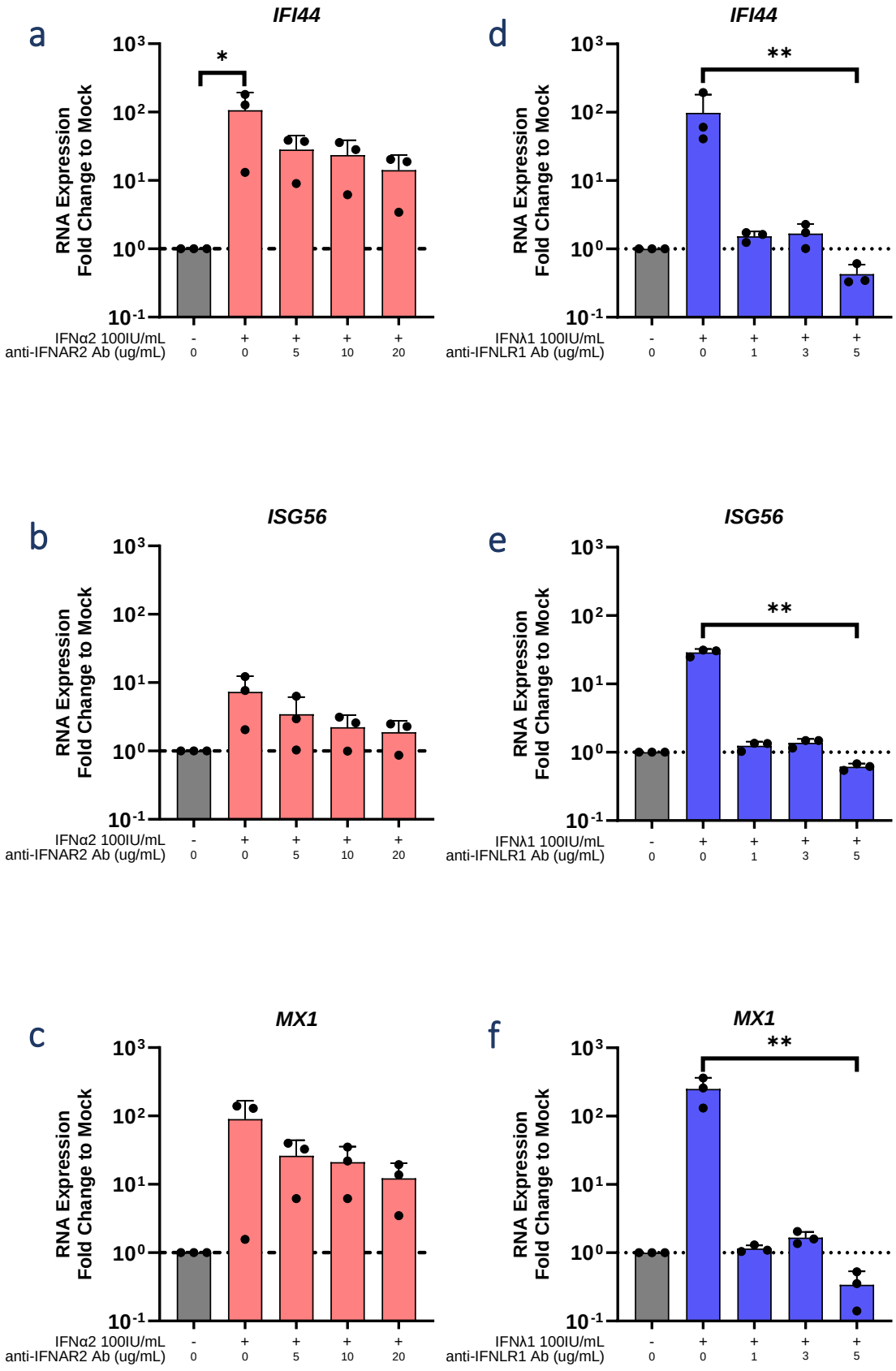

Fig. S2a-f. Inhibition of IFNα2- and IFNλ1-induced ISG expression levels by anti-IFNAR and anti-IFNLR Abs. a-f) A549 cells were treated with anti-IFNAR or anti-IFNLR Abs for 24 hours and stimulated with 100 IU/mL IFNα2, IFNλ1, or a similar volume of PBS in DMEM for 16 hours. Cells were harvested, RNA was isolated, and *IFI44* (**a**, **d**), *ISG56* (**b**, **e**), and *MX1* (**c**, **f**) mRNA expression levels were quantified by RT-qPCR. Values were normalized to unstimulated PBS-treated A549 cells.